Stellar Atmosphere

Collision

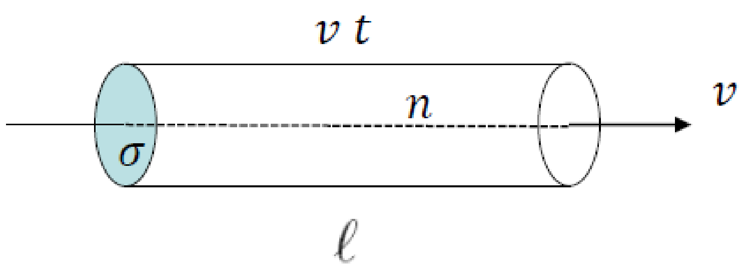

Volume V= (Area) · (length)
= cross section $\sigma \cdot \ell = \sigma\, v t$
Relative speed v
Total number of particles N
Number density $n = N/V$

# of collisions = # of (other) particles in the volume = $N = n\,(\sigma v t)$

# of collisions per unit time = $N\,/t = n\,\sigma\,v$

Time between 2 consecutive collisions (N=1) (**mean-free time**),

$$t_{\text{col}} = 1\,/\,(n\,\sigma\,v)$$

Distance between 2 consecutive collisions (N=1) (**mean-free path**),

$$\ell_{\text{col}} = v\,t_{\text{col}} = 1\,/\,(n\,\sigma\,)$$

In general "encounters" between particles, or between a particle and a photon. The "cross section" is the key.

Thermal Motion

Gas (mostly H atoms), the root-mean-squared speed

$$\frac{1}{2} m_H \sqrt{\langle v^2 \rangle} = \frac{3}{2}\, k_B\, T$$

In H I regions, $T \sim 100$ K, $\langle v \rangle_{\mathrm{H\,I}} \sim 1$ km s^{-1}, $\langle v \rangle_{e^-} \sim 50$ km s^{-1}

Cross Section

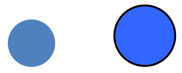

$$\sigma = \pi (a_1 + a_2)^2$$

For neutrals, hard spheres (physical cross section) OK,

$$\sigma_{\mathrm{HI,HI}} \leftarrow a \sim 5.6 \times 10^{-9}\ \mathrm{cm}$$

This is to be compared with the Bohr radius of the first orbit of $a_0 = 5.3 \times 10^{-9}$ cm

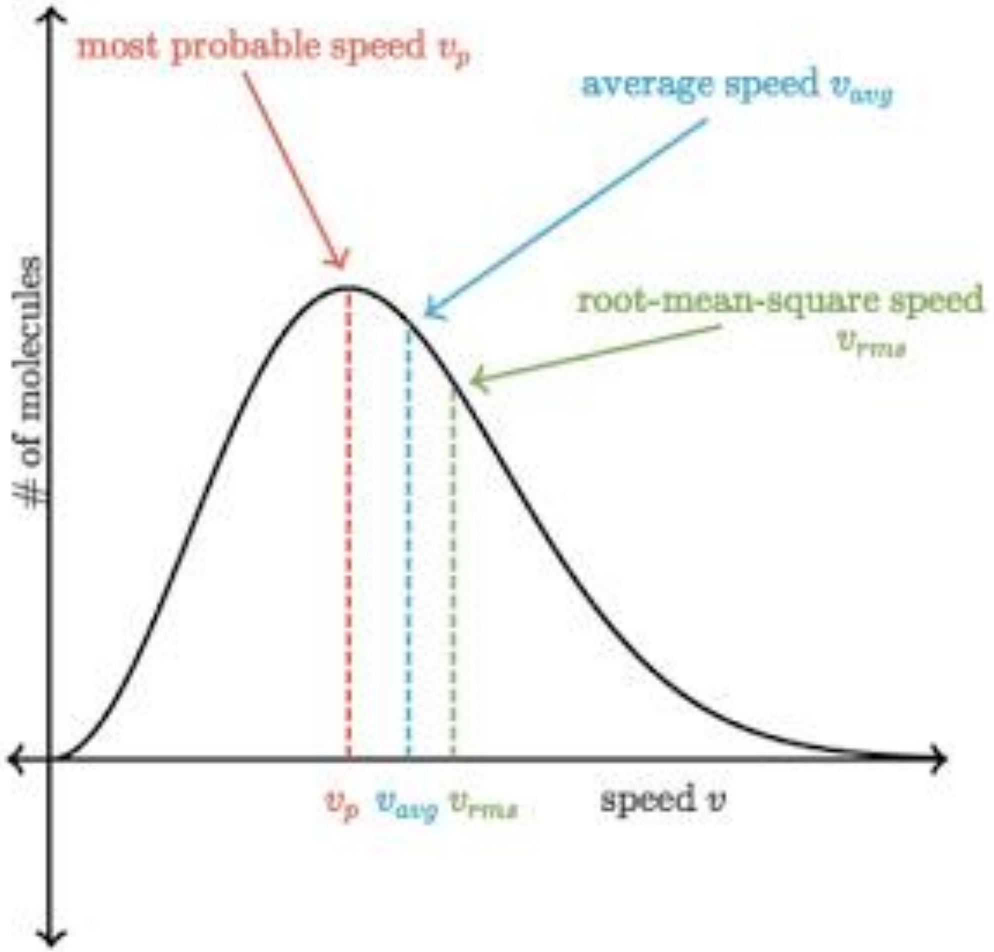

$$v_{\mathrm{mp}} = \sqrt{\frac{2\,k_B\,T}{m}}$$

$$\langle v \rangle = \sqrt{\frac{8\,k_B\,T}{\pi\,m}}$$

$$v_{\mathrm{rms}} = \sqrt{\frac{3\,k_B\,T}{m}}$$

In an HI cloud, $n_{HI} \sim 10\ \mathrm{cm}^{-3}$; $v_{HI} \sim 1\ \mathrm{km\ s}^{-1}$; $\sigma_{HI,HI} \sim 10^{-16}\ \mathrm{cm}^2$

$$t_{HI,HI} \sim 10^{10}\ \mathrm{s} \sim 300\ \text{years};\ \ell \sim 10^{15}\ \mathrm{cm} \sim 100\ \mathrm{au}$$

$\therefore$ Collisions are indeed very rare.

$$\sigma_{HI,\,e^-} \sim 10^{-15}\ \mathrm{cm}^2\ \text{(polarization)}$$

$$t_{HI,\,e^-} \sim (10 \times 10^{-15} \times 10^5)^{-1} \sim 10^{10}\ \mathrm{s} \sim 30\ \text{years}$$

$$\sigma_{e^-,\,e^-} \sim 10^{-12}\ \mathrm{cm}^2;\ n_e \sim 0.2\ \mathrm{cm}^{-3}$$

$$t_{HI,\,e^-} \sim 10^{10}\ \mathrm{s} \sim 10\ \text{days}$$

Cross Section (*cont.*)

For free e^- and p^+, $\sigma \gg \ \sigma_{\text{physical},}$ because of the Coulomb force

$\Longrightarrow$ Need QM, $a\sim 2.5 \times 10^{-2}/v^2_{\text{km/s}}$ [cm]

If $v_{e^-} \sim$ 50 km s^{-1}, $a\sim 10^{-5}$ cm for e^--e^- encounters

If $T = 3 \times 10^4$ K, $\langle v \rangle \sim 10^3$ km s^{-1} $\longrightarrow a\sim 2.5 \times 10^{-8}$ [cm]

c.f., the classical electron radius $r_e = \dfrac{e^2}{m_e\, c^2} = 2.82 \times 10^{-13}$ [cm]

Conventional unit: 1 barn $= 10^{-24}$ [cm^2]

$\sigma_{HI,HI} \sim 10^{-16}$ cm$^2 \sim 10^8$ barns

Opacity

$$\kappa\ [\mathrm{cm}^{-1}] = \kappa'\rho\ [\mathrm{cm}^2\ \mathrm{g}^{-1} \cdot\ \mathrm{g\ cm}^{-3}] = \sum_i n_i\, \sigma_i = {}^{1}\!/_{\ell}$$

Recall that $\int \kappa\, ds$ is the optical depth.

If κ_ν is frequency independent → κ, e.g., **gray atmosphere**

Usually an average opacity is used.

$$\kappa_\mathrm{P} = \frac{\int \kappa_\nu\, B_\nu\, d\nu}{\int B_\nu\, d\nu}$$

Planck opacity → average of frequency dependent opacity weighted by Planck function

Rosseland opacity Svein Rosseland → weighted by the T derivative, averaging $1/\kappa_\nu$

$$1/\kappa_\mathrm{R} = \frac{\int {\kappa_\nu}^{-1}\, u_\nu\, d\nu}{\int u_\nu\, d\nu}$$

$$u(\nu, T) = \partial B_\nu(T)/\partial T$$

Svein Rosseland - Wikipedia
en.wikipedia.org/wiki/Svein_Rosseland
YouTube 地圖 an invite to join a... 收件匣 (36) - wenp...

Svein Rosseland

Contents [hide]

From Wikipedia, the free encyclopedia

This article is about the Norwegian physicist. For the asteroid named after him, see 1646 Rosseland.

Svein Rosseland (March 31, 1894, in Kvam, Hardanger – January 19, 1985, in Bærum) was a Norwegian astrophysicist and a pioneer in the field of theoretical astrophysics.[1]

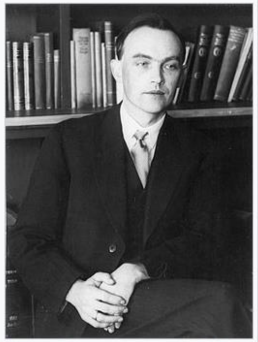

Svein Rosseland, ca. 1935

Biography [edit]

Svein Rosseland was born in Kvam, in Hardanger, Norway.[2] Rosseland grew up the youngest of nine siblings. He went to his final exams in Haugesund in 1917 and then went to the University of Oslo. After only three semesters at the University he left in 1919 to work as an assistant professor with the meteorologist Vilhelm Bjerknes at the Bergen School of Meteorology. In 1920 he went to the Institute of Physics (now the Niels Bohr Institute) in Copenhagen, where he met Niels Bohr and other prominent physicists, and where he wrote two seminal papers. He spent 1924–1926 as a Rockefeller Fellow at the Mount Wilson Observatory in Pasadena, California.[3]

In 1927, Rosseland earned a PhD. from the University of Oslo. As a professor at the University of Oslo from 1928 to 1964, he built up and headed academics at the Institute of Theoretical Astrophysics (*Institutt for Teoretisk Astrofysikk*). Rosseland was a key participant when the University of Oslo built the Institute of Theoretical Astrophysics in 1934, using funding from the Rockefeller Foundation. Between 1929-30 he was a guest professor at the Harvard College Observatory. In 1934 he founded the journal *Astrophysics Norvegica*, published by the Norwegian Academy of Science and Letters. In 1936 he published his textbook *Theoretical Astrophysics*, which contained numerous original contributions. Rosseland was instrumental in the effort behind the building of the Oslo Analyzer, finished in 1938 and for four years the world's most powerful differential analyzer.[4][5]

With the German occupation of Norway in World War II, he fled the country and went to the United States, where he was appointed a professor at Princeton University. In 1943 he went to London to work with the development of radar by the British Air Defense Ministry and later at the Admiralty, where he worked on underwater explosions. He was also a consultant for the U.S. Time Corporation, a company that later evolved into the Norwegian-owned company Timex Group USA. In the war's final years, he worked on military research at Columbia University.[6]

Rosseland returned to Norway in 1946. In the postwar period he was involved in the development of the Norwegian research policy and was among those involved in the creation of the Institute for Energy Technology which was established in 1948 and Norwegian Academy of Technological Sciences which was founded during 1955. He was also the driving force behind the creation of Harestua Solar Observatory located at Gunnarshaugen in Oppland, which was inaugurated in 1954.[7]

Rosseland was Norwegian delegate to the CERN Council in the early days of the organization.[8]

在這裡輸入文字來搜尋
30°C 晴 英 下午 01:39 2023/11/2

Arithmetic average, $\frac{a+b+c}{3}$, e.g., $(1+4+4)/3=3$

Geometric average, $\sqrt[3]{a \cdot b \cdot c}$, e.g., $\sqrt[3]{1 \times 4 \times 4} \approx 2.52$

Harmonic average, one of the Pythagorean means,

$$\left(\frac{1/a+1/b+1/c}{3}\right)^{-1}, \text{ e.g., } \left(\frac{1/1+1/4+1/4}{3}\right)^{-1} = 2$$

Bound-bound absorption Excitation of an electron of an atom to a higher energy state by the absorption of a photon. The excited atom then will be de-excited spontaneously, emitting a photon, or by collision with another particle.

Bound-free absorption Photoionization of an electron from an atom (ion) by the absorption of a photon. The inverse process is radiative recombination.

- **<u>Free-free absorption</u>** Transition of a free electron to a higher energy state, via interaction of a nucleus or ion, by the absorption of a photon. The inverse process is bremsstrahlung.

- **<u>Electron scattering</u>** Scattering of a photon by a free electron, also known as **Thomson** (common in stellar interior) or **Compton** (if relativistic) scattering.

- **<u>H^- absorption</u>** Important when $< 10^4$ K, i.e., dominant in the outer layer of low-mass stars (such as the Sun)

Hydrogen anion (or protide)

Opposite is H cation (or hydron or just proton)

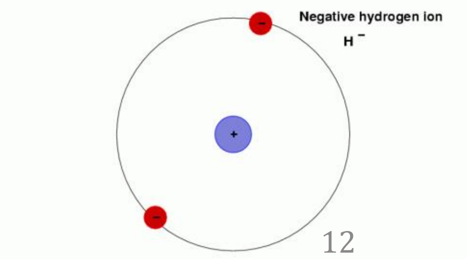

- Bound-bound, bound-free, and free-free opacities are collectively called **Kramers opacity**, named after the Dutch physicist Hendrik A. Kramers (1894-1952)
- All have similar dependence $\bar{\kappa} \propto \rho\, T^{-3.5}$; commonly used to model radiative transfer in stellar atmospheres
- Kramers opacity is the main source of opacity in gases of temperature $10^4 \sim 10^6$ K, i.e., in the interior of stars up to $\sim 1\ \mathrm{M}_{\odot}$.
- In a star much more massive, the electron scattering process dominates the opacity, and the Kramers opacity is important only in the surface layer.

Kramers opacity

$$\kappa_{Kr} \approx 4 \times 10^{25}\,(1+X)(Z+0.001)\,\rho\, T^{-3.5}\ \ [\mathrm{cm^2 g^{-1}}]$$

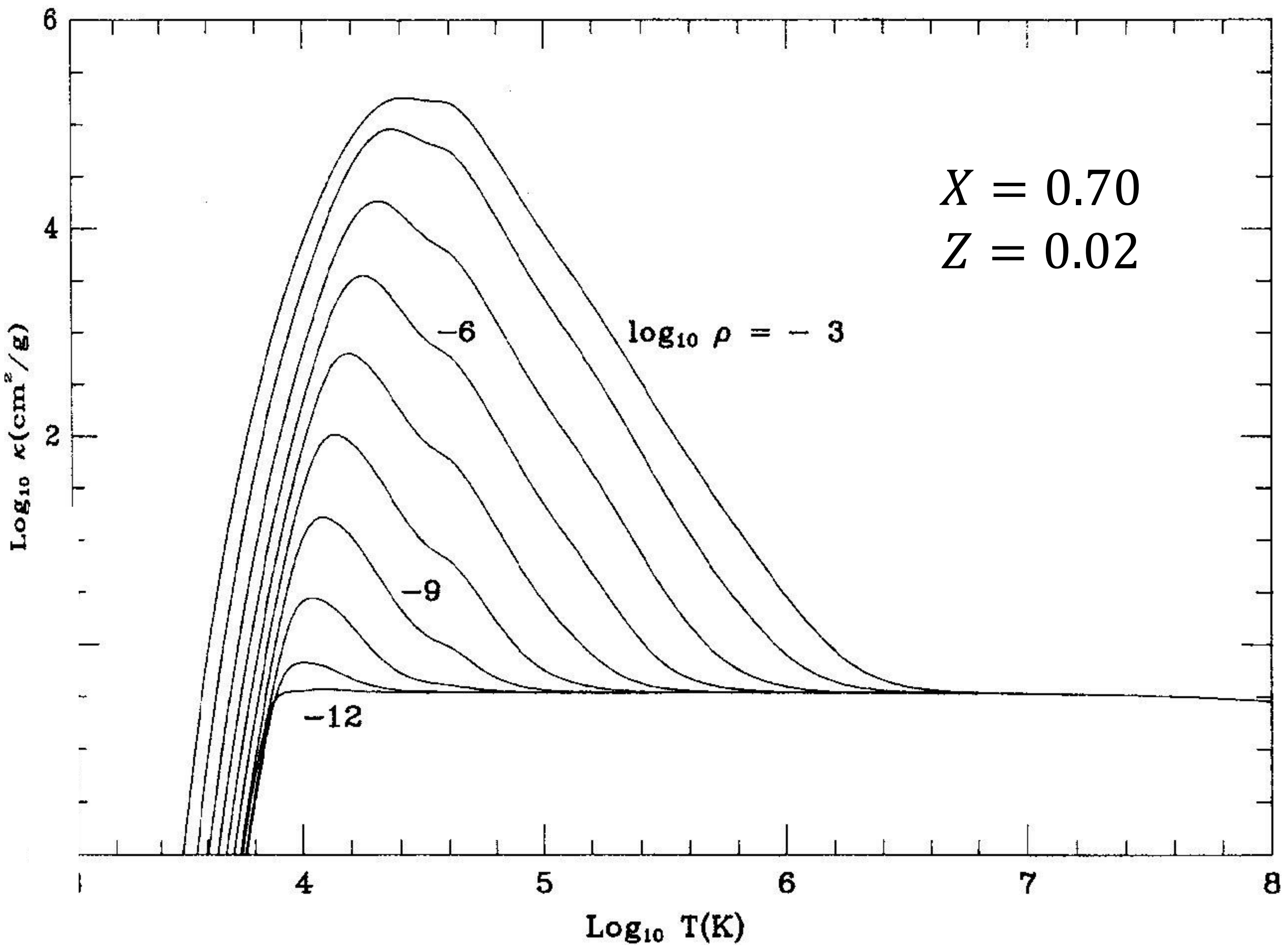

Rosseland mean opacity

Data from Iglesias & Rogers (1996)

For Thomson scattering,

$$\kappa_\nu = \frac{8\pi}{3}\frac{r_e^2}{\mu_e m_\mathrm{e}} = 0.20\,(1+X)\ \ [\mathrm{cm^2 g^{-1}}]$$

is frequency independent, so is the Rosseland mean.

$$\boxed{\kappa_{es} = 0.20\,(1+X)\ \ [\mathrm{cm^2 g^{-1}}]}$$

Here r_e is the electron <u>classical</u> (charge; Lorentz) radius,
X is the H mass fraction, and $\mu_e = 2/(1+X)$

$$\boxed{r_e = \frac{e^2}{mc^2} = 2.82 \times 10^{-15}\ [\mathrm{m}];\ \text{experimentally}\ r_e < 10^{-18}\ [\mathrm{m}]}$$

Classical electron (Thomson) cross section,

$$\sigma_\mathrm{T} = 6.65 \times 10^{-25}\ [\mathrm{cm^2}] = 0.665\ \text{barns}$$

1 femtometer (fm) = 10^{-15}m
1 barn = 10^{-28} m^2

$r_\mathrm{e} = 2.82$ fm
$r_\mathrm{proton} = 1.11$ fm

- For H^- opacity, $E_{\text{ion}} = 0.754$ eV; photons $\lambda < 16400$ Å can ionize the H^- ion. Important for $4 \times 10^3 \lesssim T \lesssim 8 \times 10^3$ K

Solar photosphere!

$$\kappa_{H^-} \approx 2.5 \times 10^{-31} \left(\frac{Z}{0.02}\right) \rho^{0.5} T^9 \ [\text{cm}^2 \ \text{g}^{-1}]$$

is temperature and metallicity (providing electrons) dependent.

- For $T \gtrsim 10^4$ K, H^- is ionized → Kramers opacity

- For $T \lesssim 3500$ K, few free electrons → molecular opacity

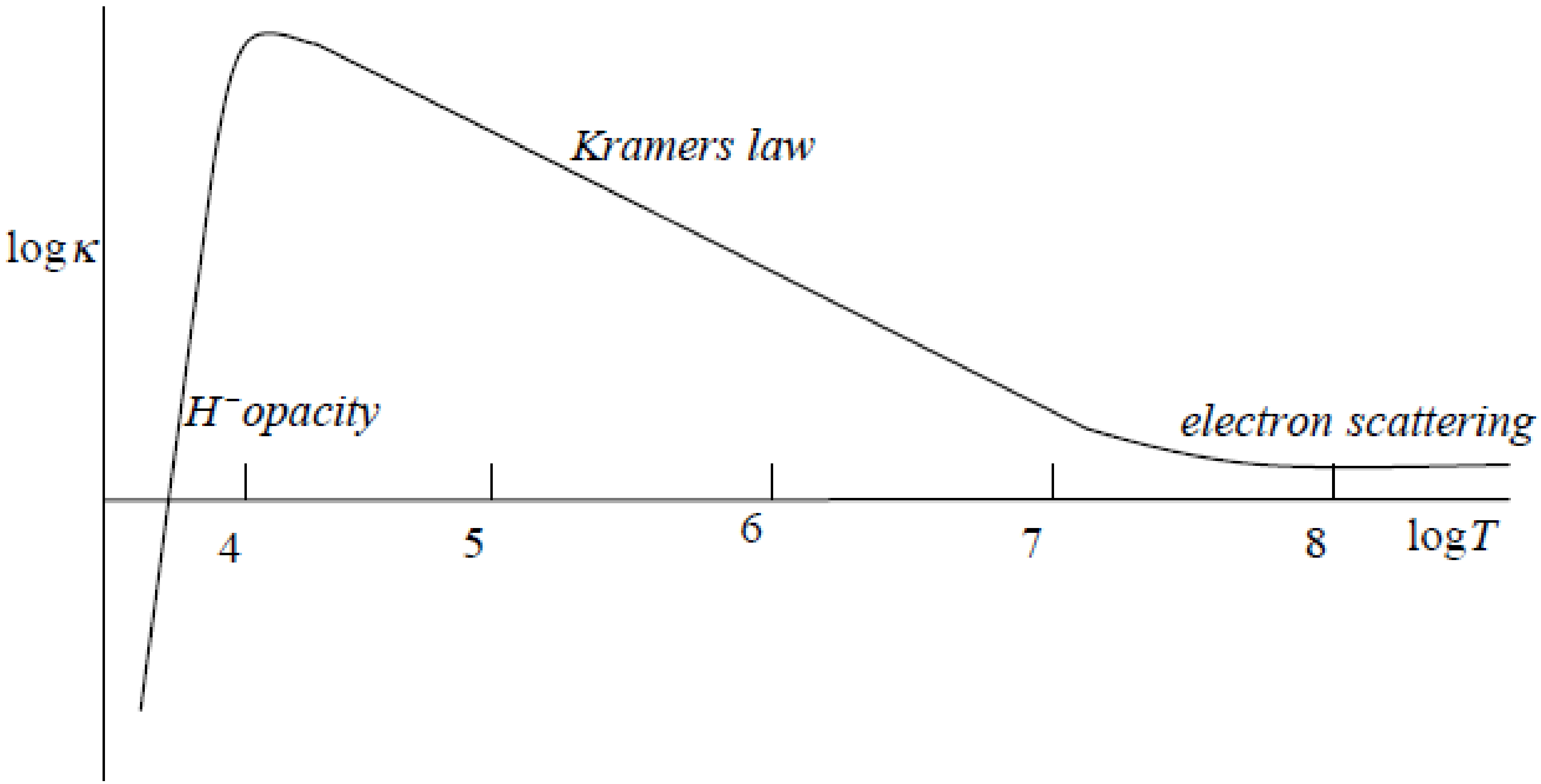

https://www.ucolick.org/~woosley/ay112-14/useful/opacityshu.pdf

The $\rho - T$ diagram

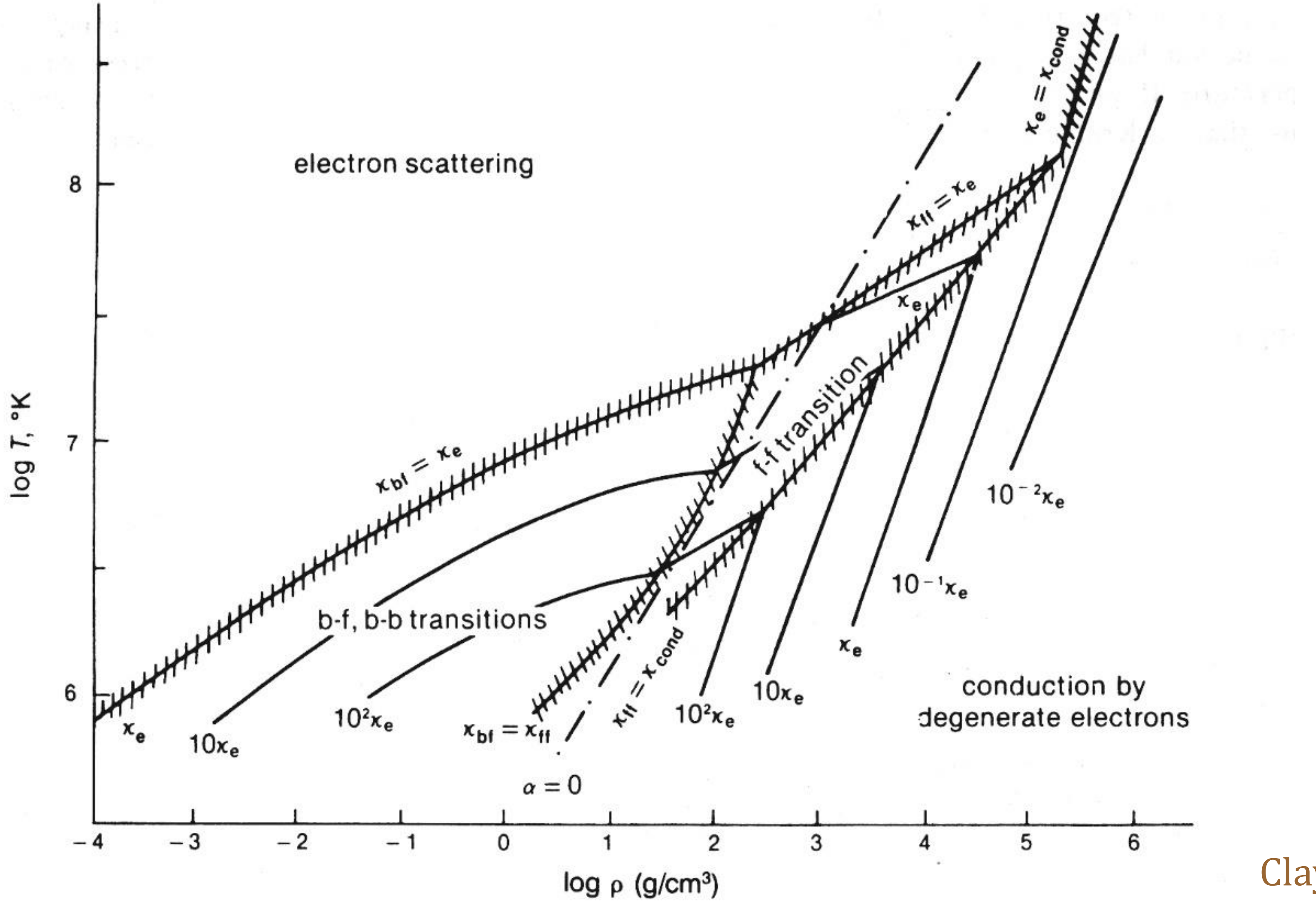

Figure 6.13. Stellar opacity in the ρ, T-plane for Population I stars. Cross-hatched lines denote boundaries at which the contributions from the two atomic process shown are equal.

Clayton Fig. Fig 3.15
Bowers & Deeming Fig 6.13

Absorption and Emission by Gas

Hydrogen as an example …

Lowest state of H, $p^2\, r^2 \approx \langle \Delta p^2 \rangle \langle \Delta r^2 \rangle \approx \hbar^2$

Virial theorem, $2\mathcal{E}_K + \mathcal{E}_p = 0$

Lowest (ground state) energy

$$\mathcal{E}_1 = -\frac{1}{2} E_p = -\frac{1}{2}\frac{Ze^2}{r} = -\frac{1}{2}\frac{p^2}{\mu} \approx -\frac{1}{2\mu}\frac{\hbar^2}{r^2}$$

μ: reduced mass

$$\frac{Ze^2}{r} = \frac{\hbar^2}{\mu r^2} \Rightarrow r = \frac{\hbar^2}{\mu Z e^2}$$ (**Bohr's radius**)

$$\mathcal{E}_1 = -\frac{1}{2}\frac{Ze^2 \mu Z e^2}{\hbar^2} = -\frac{1}{2}\frac{Z^2 \mu e^4}{\hbar^2}$$

For H, $Z = 1$, $\mathcal{E}_1 = -13.6$ eV, $r \approx 5.3 \times 10^{-9}$ [cm] $= 0.53$ Å de Broglie matter wavelength, $\lambda = \dfrac{h}{p} = \dfrac{h}{mv}$

Virial theorem (classical uniform circular motion), $mv^2 = \dfrac{Ze^2}{r}$

Standing waves, $2\pi\, r = n\lambda$

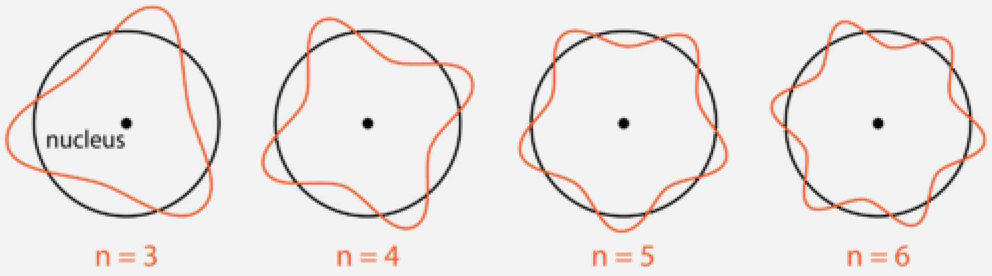

For the ground state, $n = 1, r = \dfrac{\hbar^2}{mZe^2}$

Virial theorem

relation between (the time average of) the total kinetic energy and the total potential energy of a system in equilibrium

Equation of motion (in the Lagrangian form)

$$\varrho \frac{d^2\vec{r}}{dt^2} = \vec{f} - \nabla P \;\ldots\ldots\; (1)$$

In hydrostatic equilibrium, $\frac{d^2\vec{r}}{dt^2} = 0$, so $\vec{f} = \nabla P$, and assuming spherical symmetry with the force being self-gravitation

$$\frac{dP}{dr} = -\frac{G\, m(r)\, \varrho(r)}{r^2} \quad \text{(Hydrostatic equilibrium)}$$

and $m(r) = \int_0^r 4\pi r^2 \,\varrho\, dr$ (**mass continuity/distribution**)

$\varrho \frac{d^2\vec{r}}{dt^2} = \vec{f} - \nabla P$

Take the vector dot of $\vec{r}$ of (1), divide by ϱ, define $\boldsymbol{F} = \boldsymbol{f}/\varrho$ (force per unit mass, and then integrate, using the boldface for vectors

$$\int dm\, \boldsymbol{r} \cdot \frac{\boldsymbol{d^2 r}}{\boldsymbol{dt^2}} = \int \boldsymbol{r} \cdot \boldsymbol{F}\, dm - \int \boldsymbol{r} \cdot \nabla P\, \frac{dm}{\varrho} \quad \ldots\ldots \quad (2)$$

Given $\frac{d}{dt}\left(\boldsymbol{r} \cdot \frac{d\boldsymbol{r}}{dt}\right) = \boldsymbol{r} \cdot \frac{d^2\boldsymbol{r}}{dt^2} + \left(\frac{d\boldsymbol{r}}{dt}\right)^2 = \frac{1}{2}\frac{d^2}{dt^2}\boldsymbol{r}^2$

So, $\int dm\, \boldsymbol{r} \cdot \frac{\boldsymbol{d^2 r}}{\boldsymbol{dt^2}} = \frac{1}{2}\frac{d^2}{dt^2}\int \boldsymbol{r}^2\, dm - \int \left|\frac{d\boldsymbol{r}}{dt}\right|^2 dm$

$$= \frac{1}{2}\frac{d^2 I}{dt^2} - 2\mathcal{E}_{\text{kin}}$$

I: moment of inertia

$\mathcal{E}_{\text{kin}}$: kinetic energy

Because $dm = \varrho \, dV$, the last term in (2),

$$\int \boldsymbol{r} \cdot \nabla P \, \frac{dm}{\varrho} = \int \boldsymbol{r} \cdot \nabla P \, dV = \int \nabla \cdot (\boldsymbol{r} \cdot \boldsymbol{P}) \, dV - 3 \int P \, dV$$

$$= \boldsymbol{r} \cdot \boldsymbol{P} \cdot d\boldsymbol{S} - 3 \int P \, dV$$

Note

$$\int \nabla \, (\boldsymbol{r}P) = (\nabla \cdot \boldsymbol{r})P + \boldsymbol{r} \cdot \nabla P$$

$\nabla \cdot \boldsymbol{r} = 3$

Gauss's theorem → volume integral of the divergence to surface integral

Assuming spherical symmetry,

$$= 4\pi R^3 P_s - 3 \int P \, dV$$

Putting together, we have

$$\frac{1}{2}\frac{d^2 I}{dt^2} = 2\mathcal{E}_{\text{kin}} + 3\int P\,dV + \int \boldsymbol{r}\cdot\boldsymbol{F}\,dm - \oint P\boldsymbol{r}\cdot d\boldsymbol{S}$$

where $\boldsymbol{r}\cdot\boldsymbol{F}$ (work) is virial;

or

$$\boxed{\frac{1}{2}\frac{d^2 I}{dt^2} = 2\,\mathcal{E}_{\text{kinetic}} + 3\int P\,dV + \mathcal{E}_{\text{potential}} - 4\pi R^3 P_{\text{external}}}$$

For stars, under hydrostatic equilibrium and if $P_{\text{ext}} = 0$,

$$\boxed{2\,\mathcal{E}_{\text{k}} + \mathcal{E}_{\text{p}} = 0}$$

$$\frac{1}{2}\frac{d^2 I}{dt^2} = 2\,\mathcal{E}_{\mathrm{k}} + \mathcal{E}_{\mathrm{p}}$$

LHS $= 0$ → stable

LHS < 0 → collapsing

LHS > 0 → expanding

$\mathcal{E}_{\mathrm{k}}$: a variety of kinetic energies

- ✓ Kinetic energy of molecules
- ✓ Bulk motion of clouds
- ✓ Rotation
- ✓ …

$\mathcal{E}_{\mathrm{p}}$: a variety of potential energies

- ✓ Gravitation
- ✓ Magnetic field
- ✓ Electrical field
- ✓ …

Note $\mathcal{E}_{\mathrm{total}} = \mathcal{E}_k + \mathcal{E}_p$, governs if the system is bound ($\mathcal{E}_{\mathrm{total}} < 0$)

For stars, mostly $\mathcal{E}_p = \Omega$ (gravitational energy; negative)

For higher energy states, $p_n\, r_n = n\hbar$

$$\boxed{\mathcal{E}_n = -\frac{p_n^2}{2\mu} \approx -\frac{n^2\hbar^2}{2\mu r_n^2} = -\frac{Z^2\mu\, e^4}{2n^2\hbar^2}}$$

For the n-th radial state, the phase space volume is $(4\pi p_n^2\, \Delta p_n)(4\pi r_n^2\, \Delta r_n)$, # of possible states with principle quantum number n

$$= \frac{\text{Total phase space volume}}{\text{volume of unit cell}} = \frac{16\pi^2 n^2 \hbar^3}{\hbar^3} \propto n^2$$

The electron spin is either parallel or anti-parallel to that of the nucleus, so the n-th state has $2n^2$ different substates (degeneracy), all having the same energy.

$$\mathcal{E}_n = -\frac{Z^2 \mu\, e^4}{2n^2 \hbar^2}$$

Note that $\mathcal{E}_n \propto \mu$

For normal H, $\mu_H = \frac{m_e m_p}{m_e + m_p} = \frac{m_e}{1 + m_e/m_p} \approx m_e(1 - m_e/m_p)$

For deuteron, $\mu_D = \frac{m_e m_D}{m_e + m_D} = \frac{2 m_e m_p}{m_e + 2m_p} \approx m_e(1 - m_e/2m_p) > \mu_H$

So the D lines are 1.5 Å shorter in wavelengths

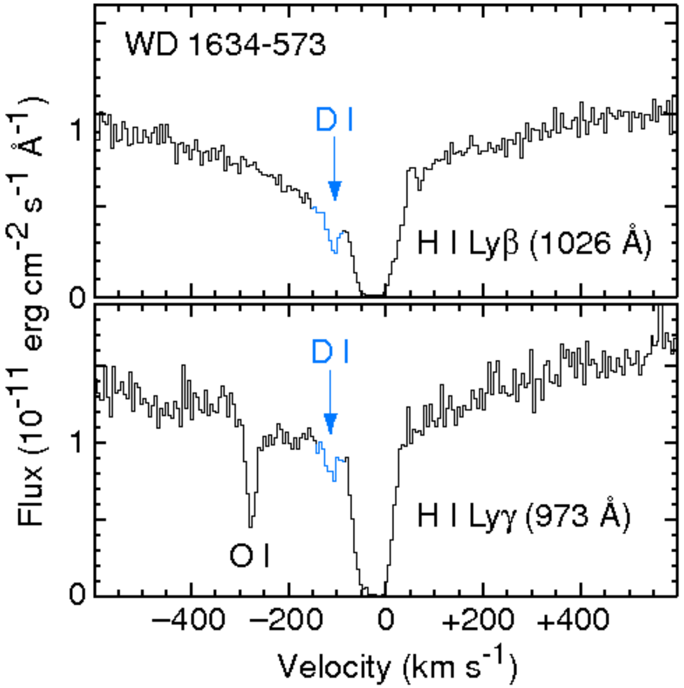

Note also that $\mathcal{E}_n \propto Z^2$, so for He II ($Z = 2$, with 1 e$^-$), Z^2 is 4 times larger, and with a different μ.

https://archive.stsci.edu/fuse/scisumm/sci_d2h.html

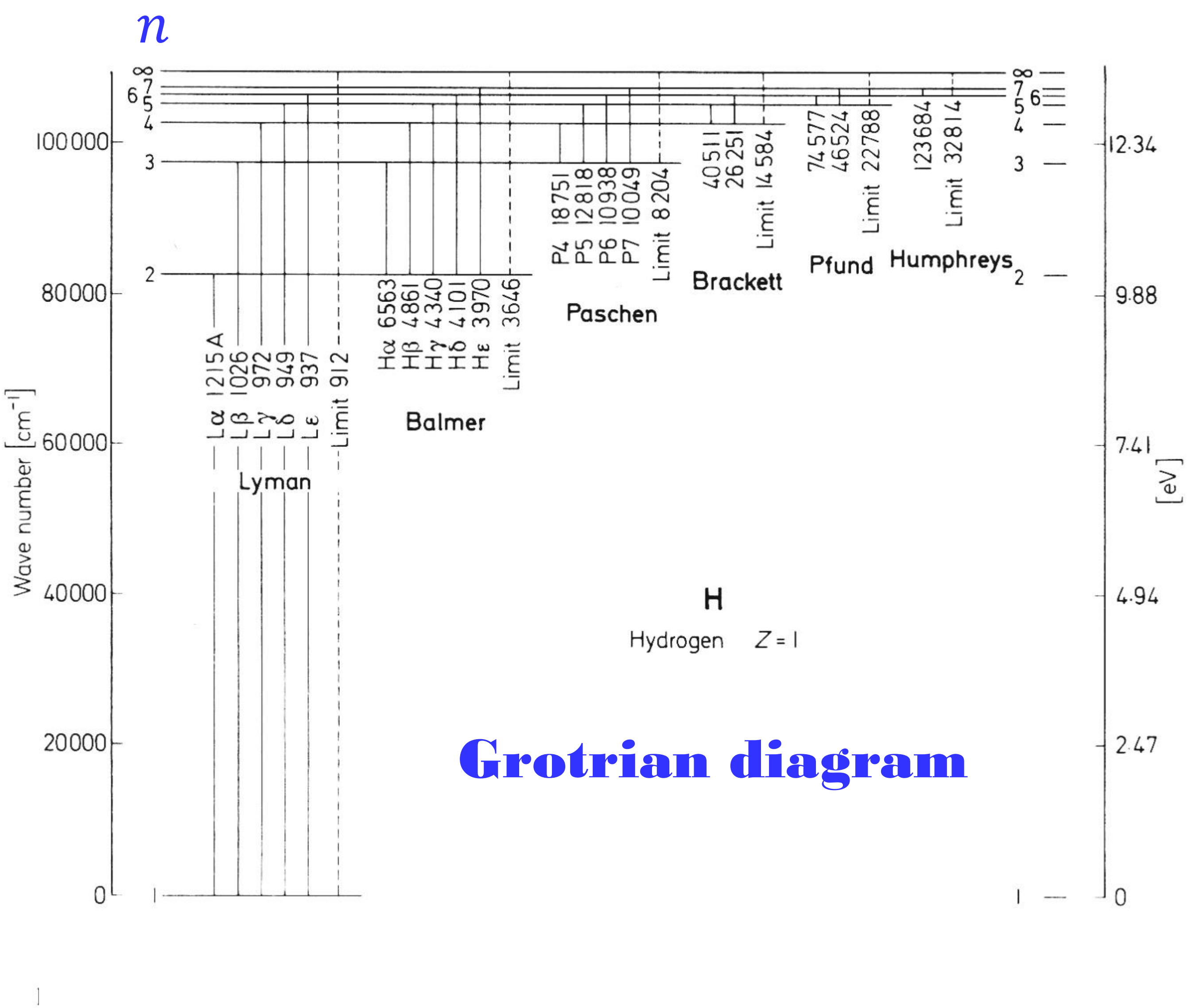

Lang

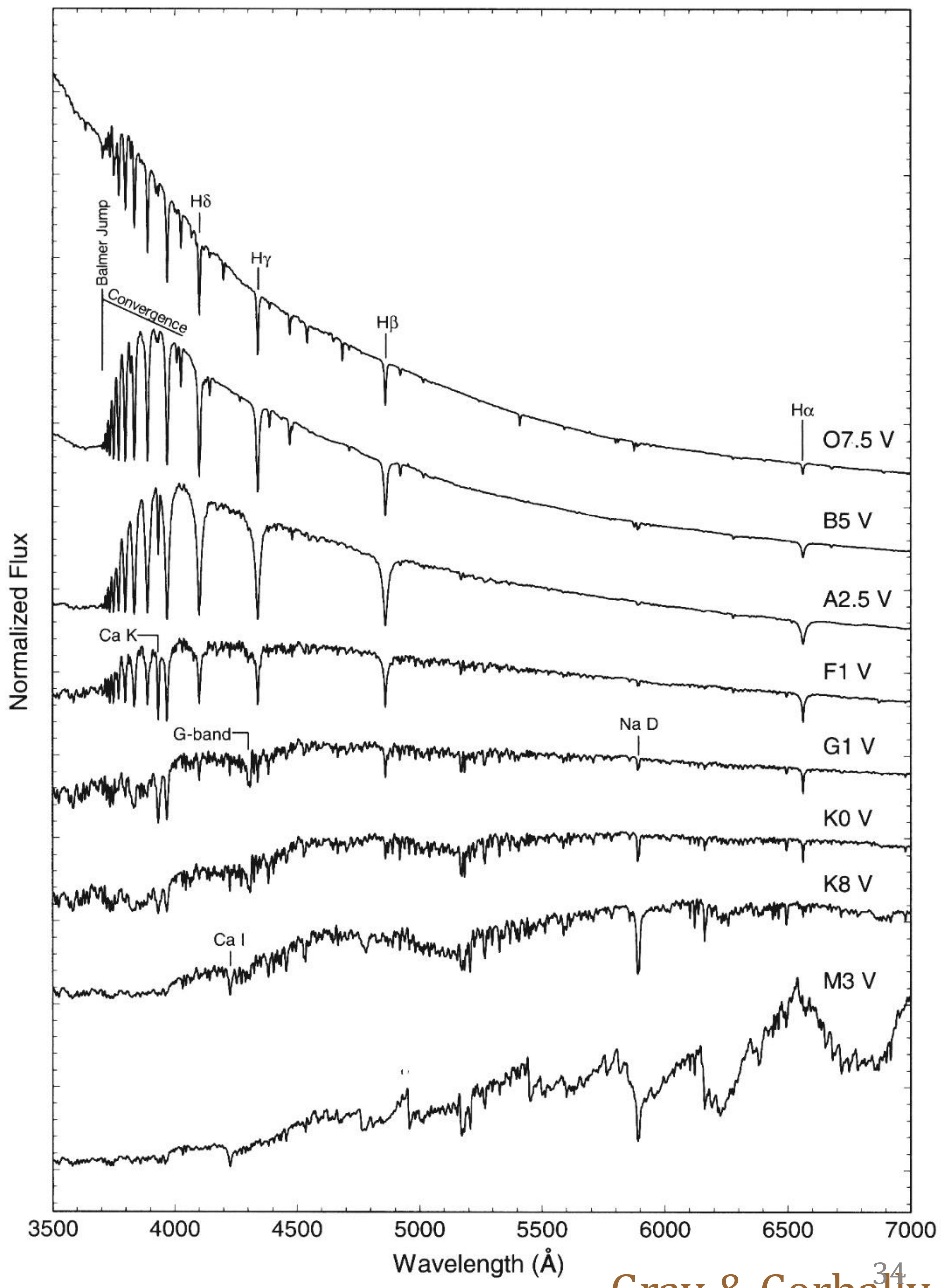

Gray & Corbally

- For the ground state, the orbital angular momentum is $\ell = 0$. The total spin angular momentum is

$$F = 0 \text{ (spin opposite) or } F = 1 \text{ (spin parallel)}$$

Hyperfine splitting

- For $n = 2$, ℓ =1, and with spin, a total angular momentum of $\ell(\ell+1)\hbar^2$ =$2\hbar^2$

  3 substates, $\hbar, 0, -\hbar$, $m = 1, 0, -1$ (magnetic quantum number)

  Fine structure, $\Delta\mathcal{E}$ very small, $\sim 10^{-5}$ Ev

  But if there is an external **B** field → Zeeman splitting

H^+

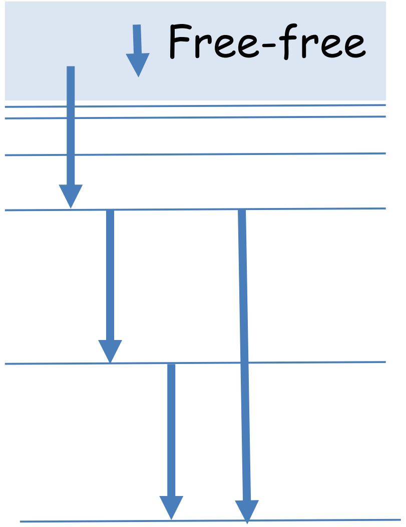

- Free-free or free-bound to any level
- Cascading down → emission of photons of different energies

H^-

$$H + e^- \longrightarrow H^- + h\nu$$

Proton-electron is polarized.

Stars: ample supplies of free e^- from Na, Ca, Mg, … with low-ionization potentials

- He atom similar, with the second e^- weakly bound, shielded by the first e^-
- $\mathcal{E}_{\text{binding}}(\mathrm{H}^-) = 0.75$ eV, only 1 bound state; transitions → continuum
- Absorption by H^- immediately followed by reemission

The sunlight we see mostly is due to continuum transitions by H^-

H_2

- Main constituent of cold clouds, not important in stars, except in the coolest substellar objects (brown dwarfs or planetary-mass objects)
- Lacking a permanent electric dipole moment, so very difficult to detect. A rotationally excited molecule would radiate through a relatively slow electric quadrupole transition.
- Only detected in a hot medium, where stellar radiation or stellar wind excites vibrational and electronic states which then decay relatively quickly.

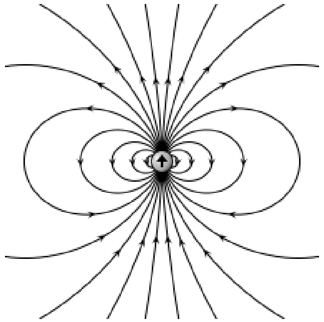

Zero electric dipole moment

◆Electric dipole moment $\vec{p} = q\vec{d}$

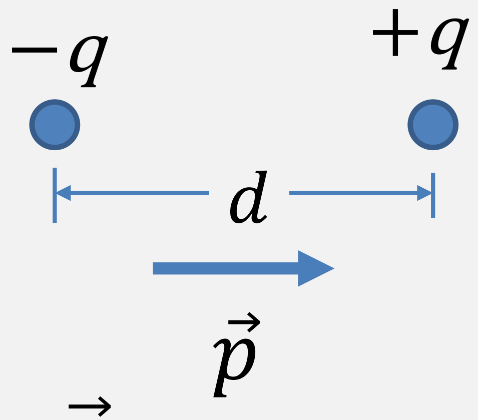

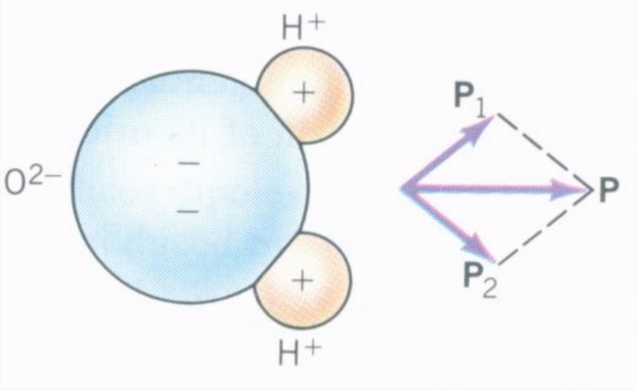

✓ With more than one dipole, the net dipole moment is the vector sum of all individual moments.

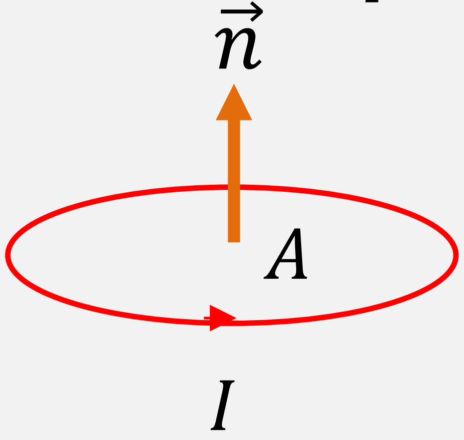

◆Magnetic dipole moment $\vec{\mu} = IA\vec{n}$

◆Electric quadrupole moment

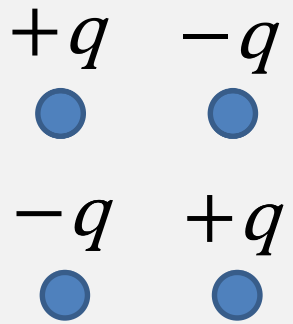

$$\vec{q} = \begin{pmatrix} q_{xx} & q_{xy} & q_{xz} \\ q_{xy} & q_{yy} & q_{yz} \\ q_{xz} & q_{yz} & q_{zz} \end{pmatrix}$$

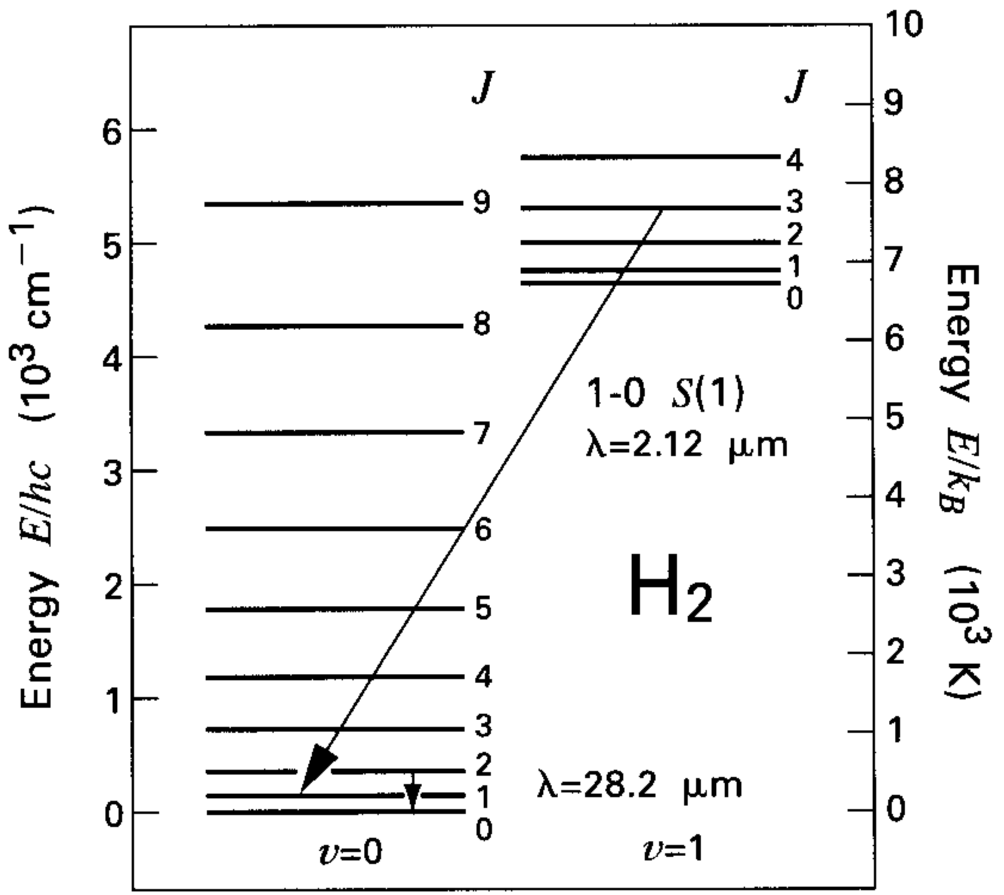

Figure 5.4 Rotational levels of H_2 for the first two vibrational states. Within the $v = 0$ state, the $J = 2 \rightarrow 0$ transition at 28.2 μm is displayed. Also shown is the transition giving the 1-0 S(1) rovibrational line at 2.12 μm. Note that two different energy scales are used.

Stahler & Palla

CO molecules

- Simple and abundant, in gaseous or solid form
- Strong $\mathcal{E}_{\text{binding}}$ =11.1 eV → self-shielding against UV field
- with a permanent electric dipole moment; radiating strongly at radio frequencies.
- $^{12}C^{16}O$ easiest to detect; isotopes $^{13}C^{16}O$, $^{12}C^{18}O$, $^{12}C^{17}O$, $^{13}C^{18}O$ also useful
- Low critical density for excitation → CO used to study the <u>large-scale distribution</u> of molecules, as a tracer of H_2 in dense clouds
- $^{12}C^{16}O$ almost always optically thick; same line from other rare isotopes usually not → estimate of column density (total mass) of molecular gas $N_H = 10^6\, N_{^{13}CO}$

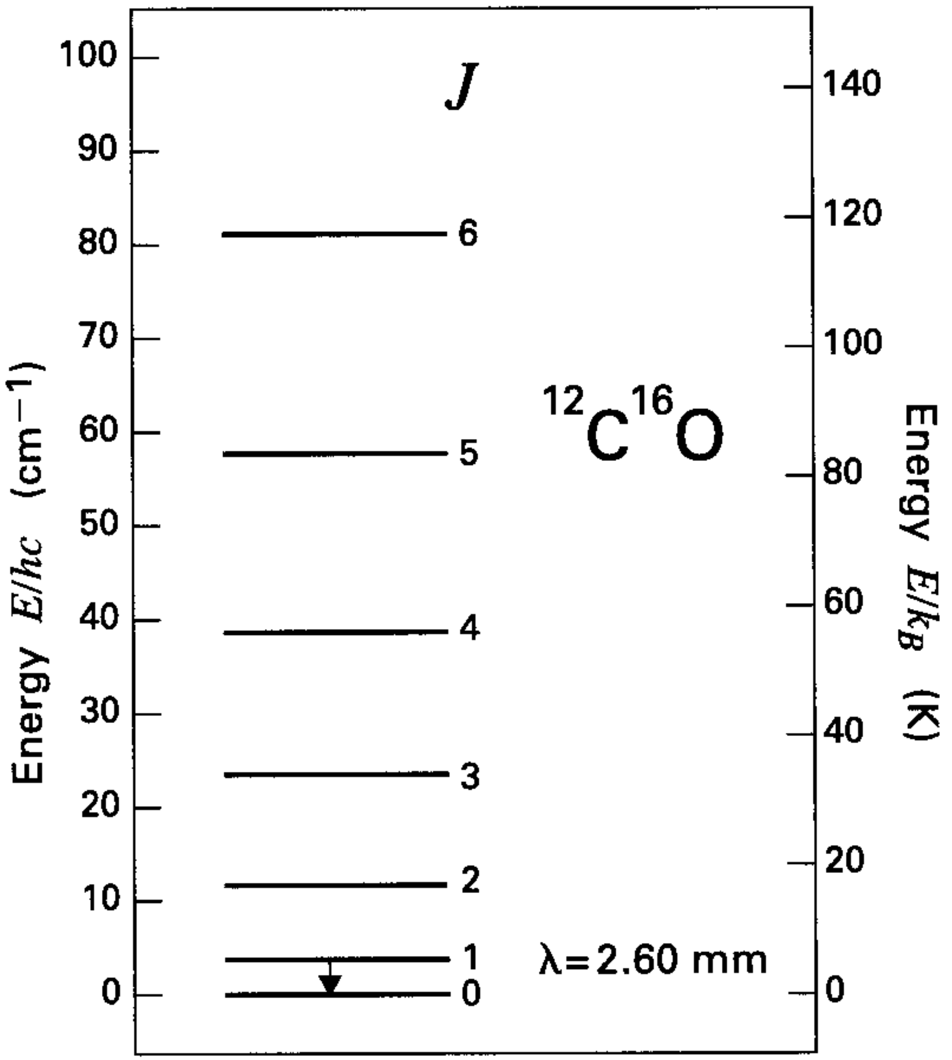

Figure 5.6 Rotational levels of $^{12}C^{16}O$ within the ground ($v = 0$) vibrational state. The astrophysically important $J = 1 \to 0$ transition at 2.60 mm is shown.

2.6 mm = 115 GHz

Only 5 K above the ground level … can be excited by collisions with ambient molecules or CMB photons

Stahler & Palla

Molecules in stars

- Stellar matter largely gas or plasma.
- Molecules form primarily below 6000 K, only OB stars do not contain molecules.
- Absorption band spectra, e.g., due to MgH, CaH, FeH, CrH, NaH, OH, SiH, VO, and TiO, etc.
- Late-type stars exhibit TiO
- NH_3 and collision-induced absorption by H_2 in brown dwarfs or in planet-mass objects

CO bandheads in the Becklin-Neugebauer (BN) object, an IR-emitting, embedded, massive (~7 $M_\odot$) protostar

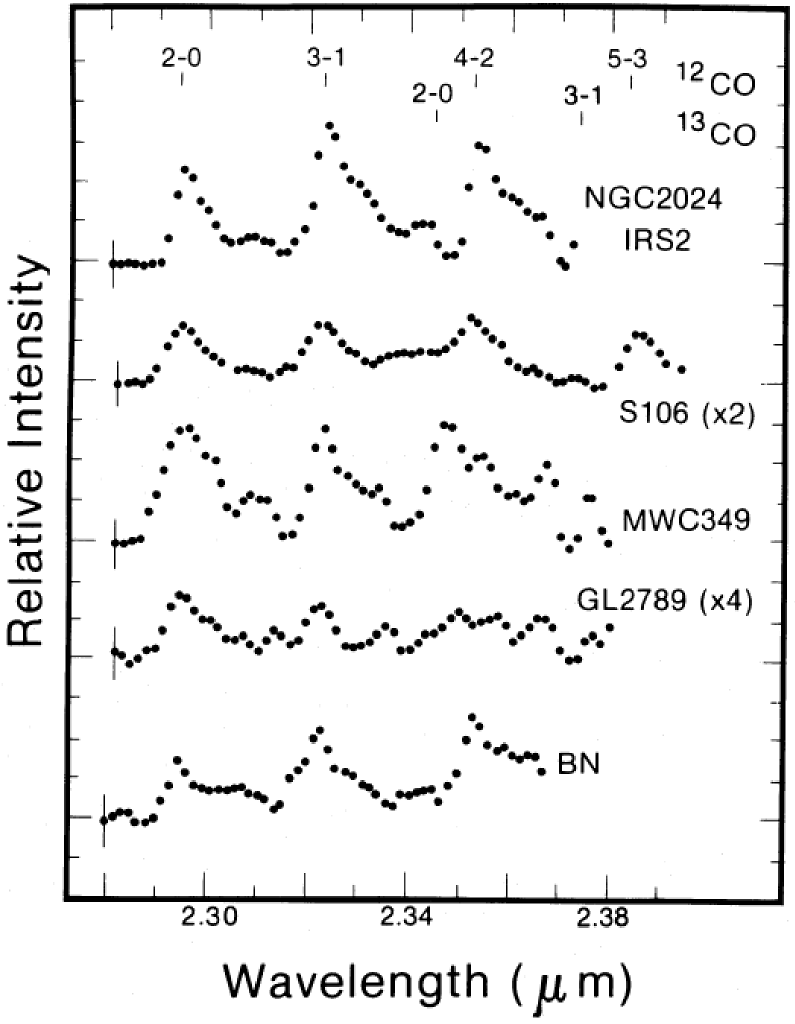

FIG. 2.—Spectra of those sources in which CO band head emission was detected. Linear baselines have been subtracted from each spectrum. The positions of the band heads are indicated at the top of the figure. Vertical scale marks are separated by 2×10^{-17} W cm^{-2} μm^{-1}. Noise levels are indicated on the short wavelength data points.

Gaballe & Persson (1987)

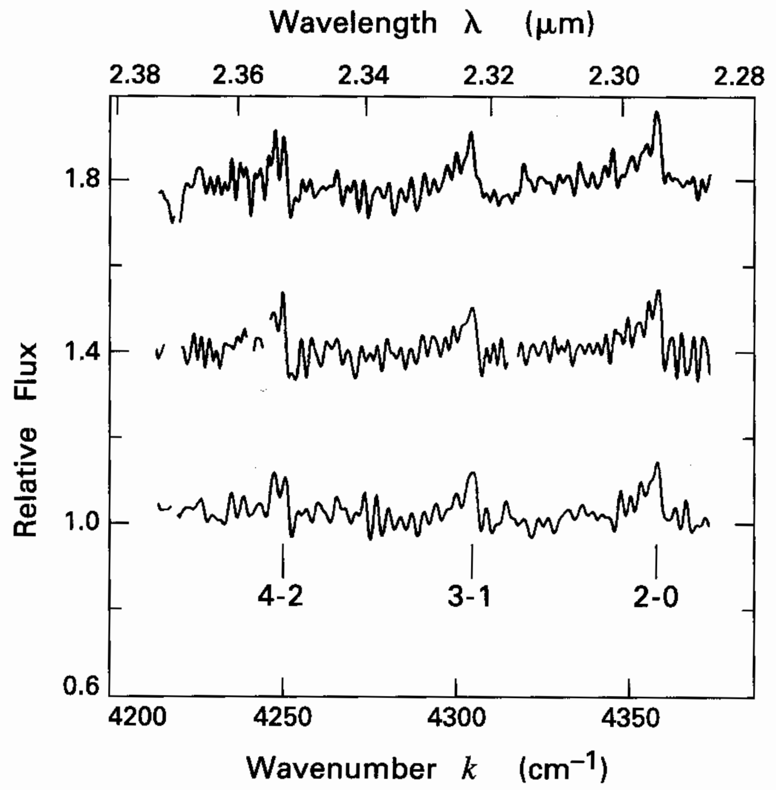

Figure 5.8 Near-infrared spectrum of the BN object in Orion, shown at three different observing times. The relative flux is plotted against the wave number k, defined here as $1/\lambda$.

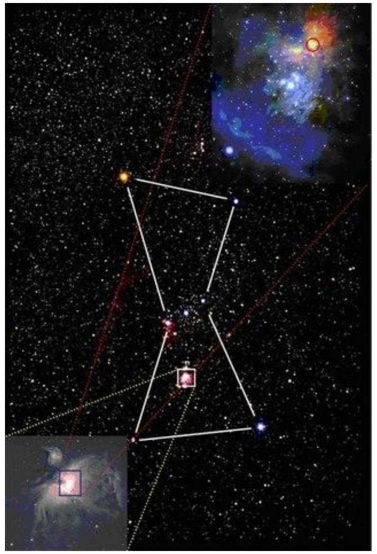

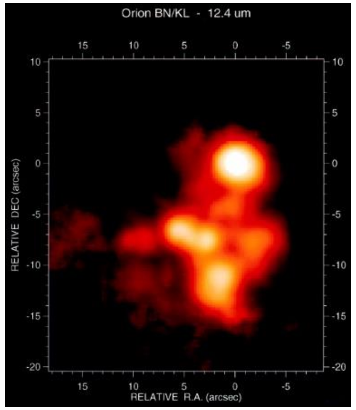

Stahler & Palla

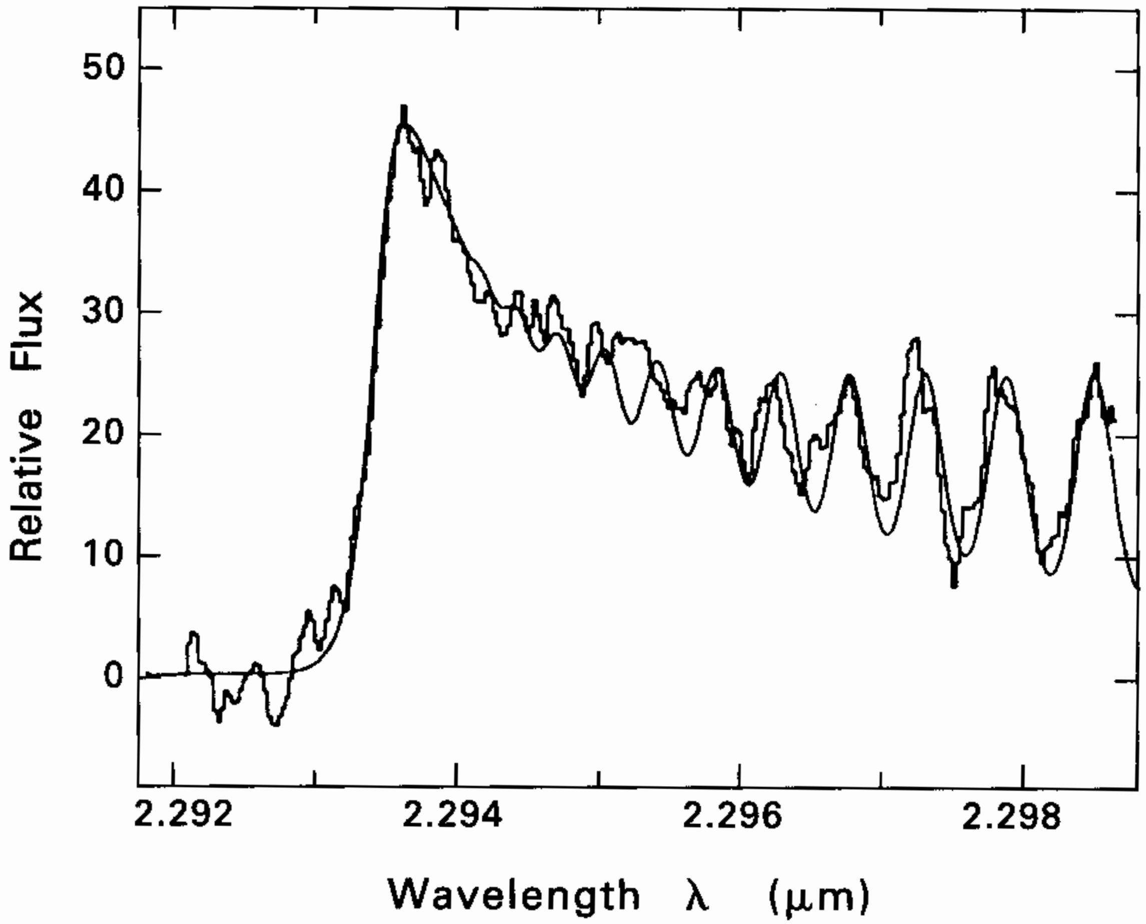

Figure 5.9 High-resolution near-infrared spectrum of the embedded stellar source SSV 13. The structure of the $v = 2 \rightarrow 0$ band head in $^{12}C^{16}O$ is evident. The smooth curve is from a theoretical model that employs an isothermal slab at 3500 K. Note that the spectrum here represents only a portion of the R-branch.

Stahler & Palla

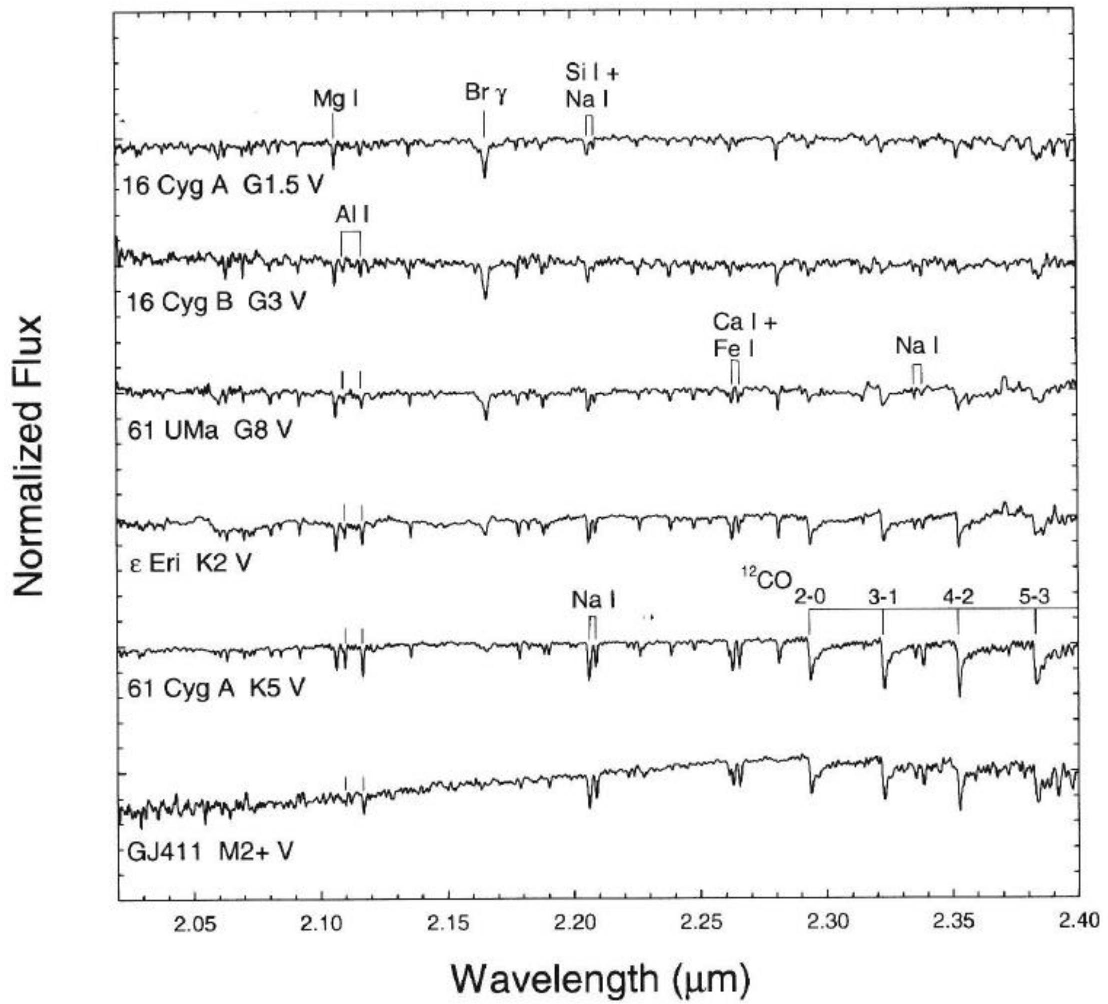

Figure 7.9 A spectral sequence for late-type dwarfs in the K-band. Brackett γ and nearby Na I and Ca I lines are marked. The spectra are from Ivanov et al. (2004) where sequences for giants, with and without metallicity effects, and for supergiants can be found.

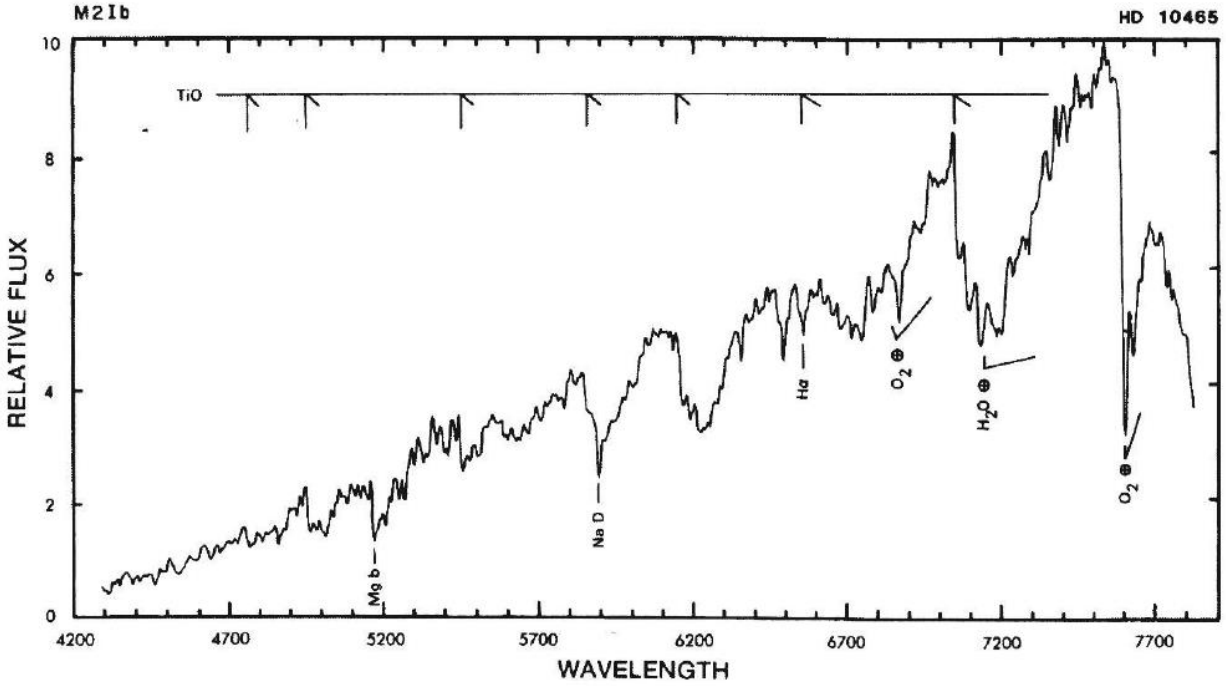

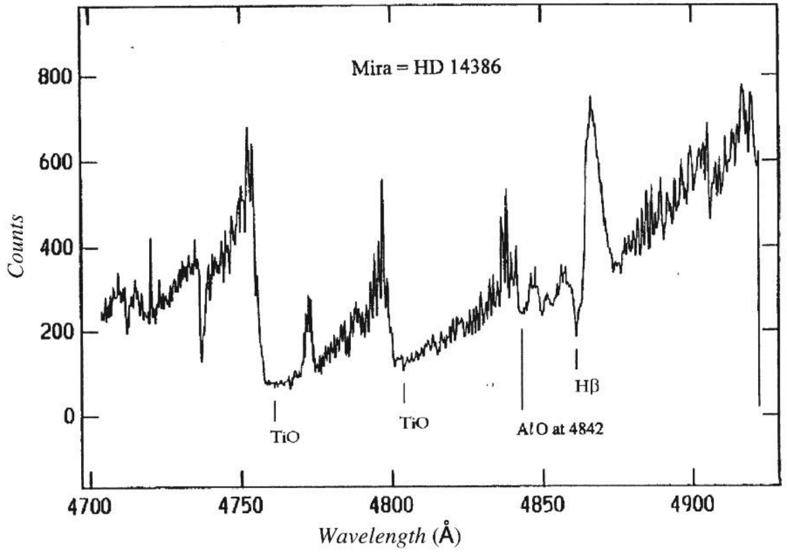

Figure 8.9 Spectrum of Mira taken in August 1966. The main AlO bandhead is at λ4842 near the mark for Hβ. Figure by kindness of Garrison (1997) and the *Journal of the American Amateur Variable Star Observers*.

Gray & Corbally

Solar Atmosphere

- **Photosphere**

  Lowest layer of the atmosphere; visible “disk”;
  thickness ~300 km (cf. 2 $R_\odot$ ~ 1.4 million km)

- **Chromosphere**

  Pinkish (hence the name);
  extending ~2500 km above the limb

- **(Transition region)**

- **Corona**

  Outermost layer; extending millions of km;
  hot (1 to 2 million K); brightness 10^{-6} photosphere;
  visible during a total solar eclipse or with a coronograph

- (**Wind**) expanding supersonically (400 km s^{-1}; 10^{-14} $M_\odot$)

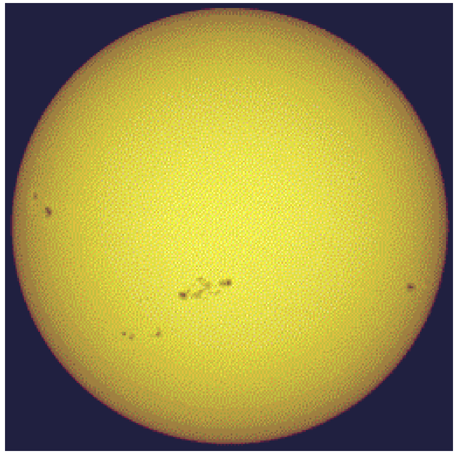

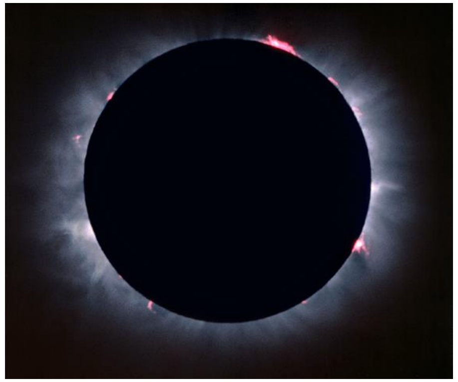

- November 15, 1999, Mercury transited, i.e., passing in front of the Sun
- Observed by the *TRACE* spacecraft
- The Sun appears larger in the ultraviolet image than in the visible-light image.

Why?

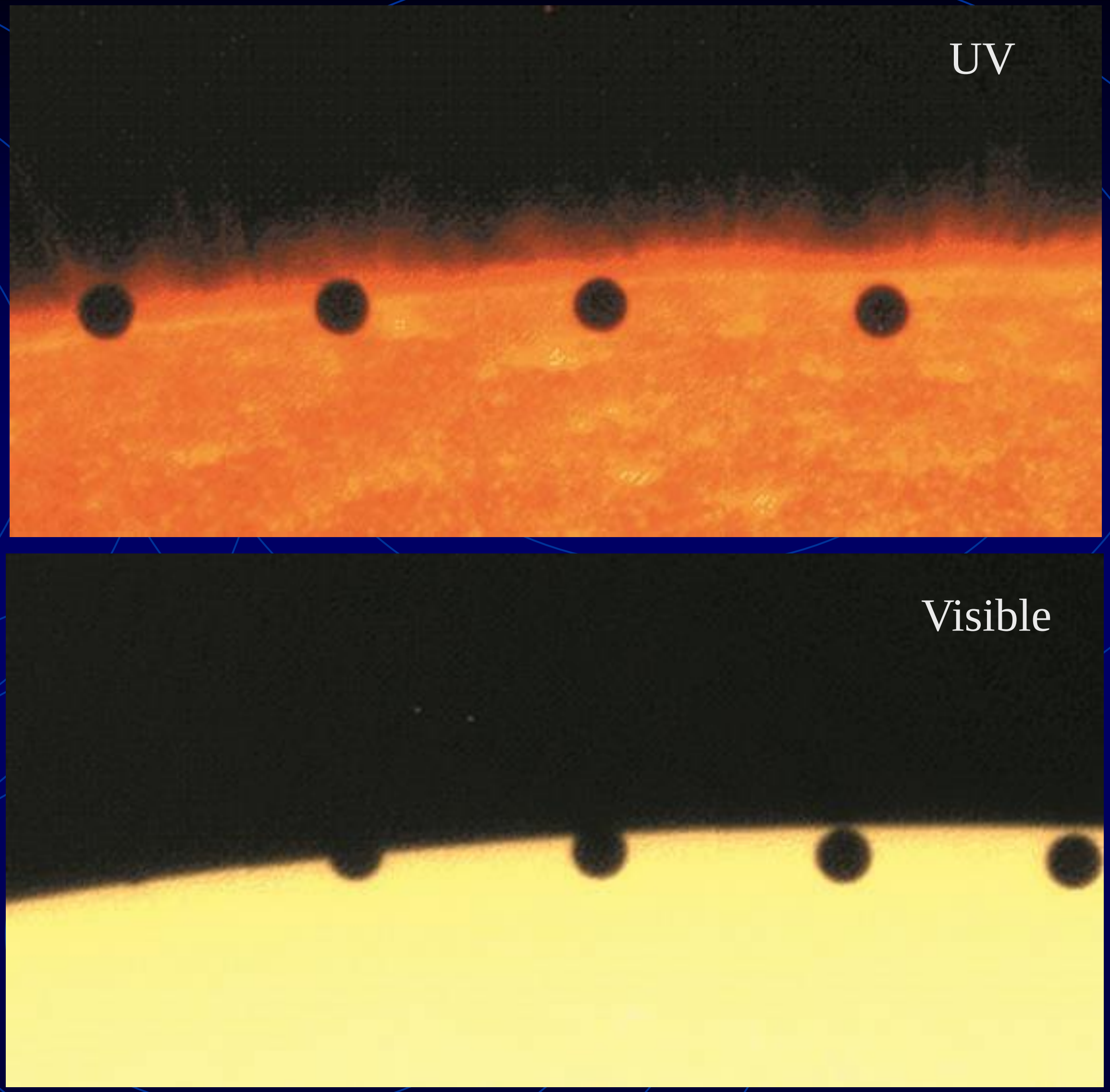

Every 6-9 min

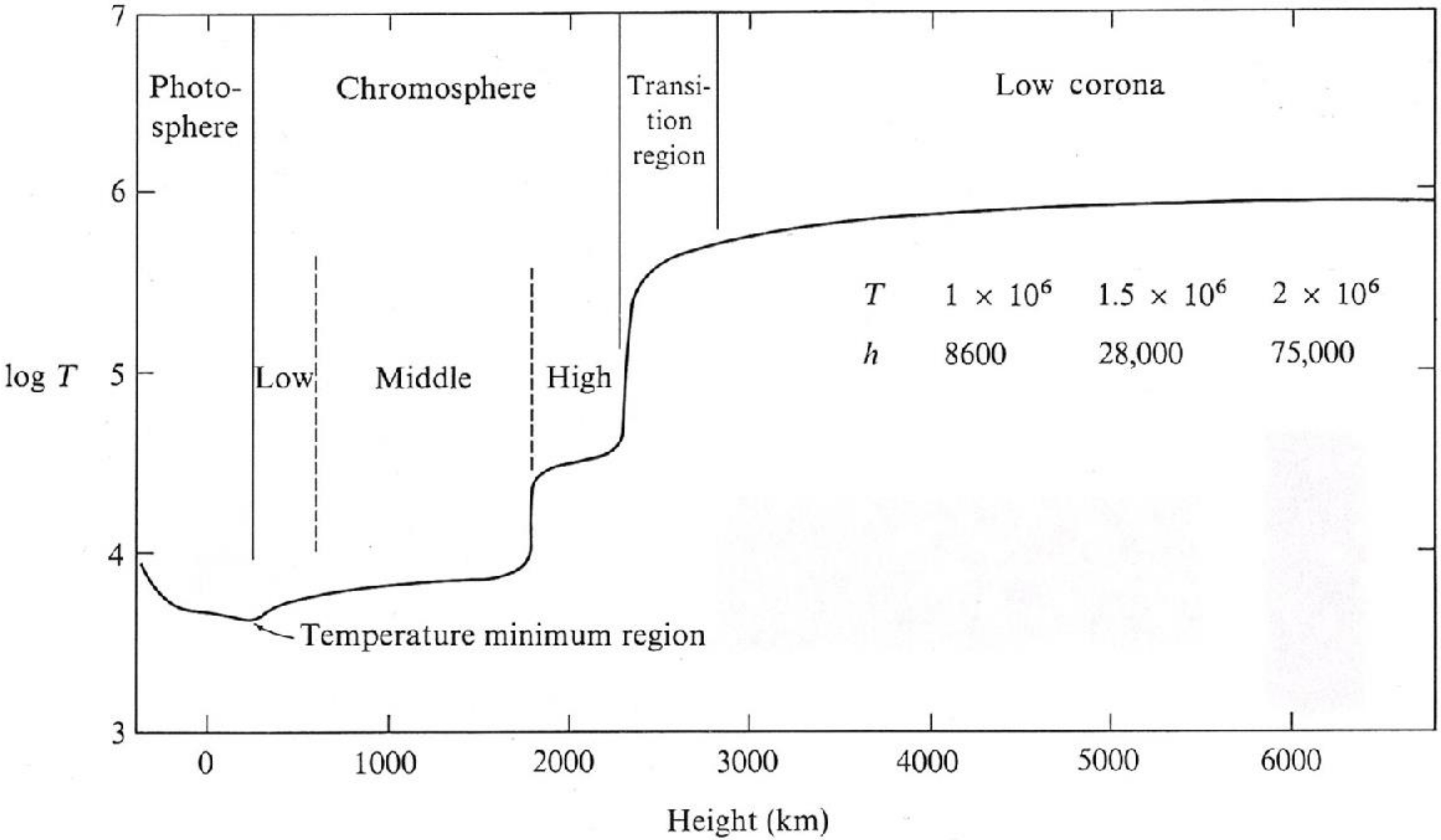

Photo-
sphere
Chromosphere
Transi-
tion
region
Low corona
Low
Middle
High
T 1 × 10^6 1.5 × 10^6 2 × 10^6
h 8600 28,000 75,000
Temperature minimum region
log T
7
6
5
4
3
0
1000
2000
3000
4000
5000
6000
Height (km)

Athay (1976)

Solar photosphere ≈ 300 km thickness ≲ 0.1% $R_\odot$

⟶ **plane parallel** approximation OK

Recall the radiative transfer equation,

$$\frac{dI_\nu}{d\tau_\nu} = I_\nu - S_\nu$$

and the <u>vertical</u> optical depth,

$$\tau_\nu(z) = \int_z^0 \kappa_\nu \, dz.$$

For a ray at an angle θ, $dz = ds\cos\theta$, so in general,

$$\boxed{\cos\theta \frac{dI_\nu(\tau_\nu,\theta)}{d\tau_\nu} = I_\nu(\tau_\nu,\theta) - S_\nu(\tau_\nu)}$$

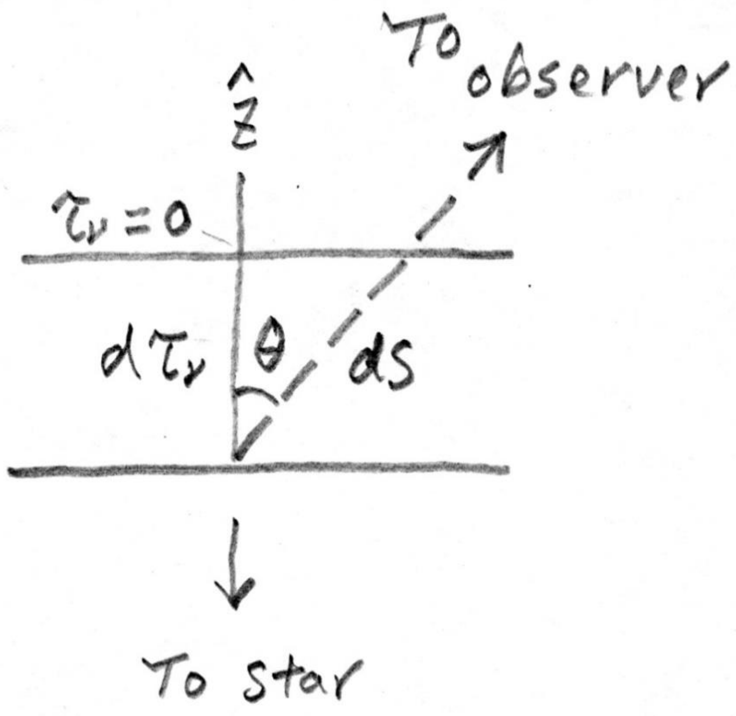

The solution then is

$$I_\nu(\tau_\nu) = I_\nu(0)\ e^{-\tau_\nu} + \int_0^{\tau_\nu} S_\nu(t_\nu)\, e^{-(\tau_\nu - t_\nu)}\, d\,t_\nu$$

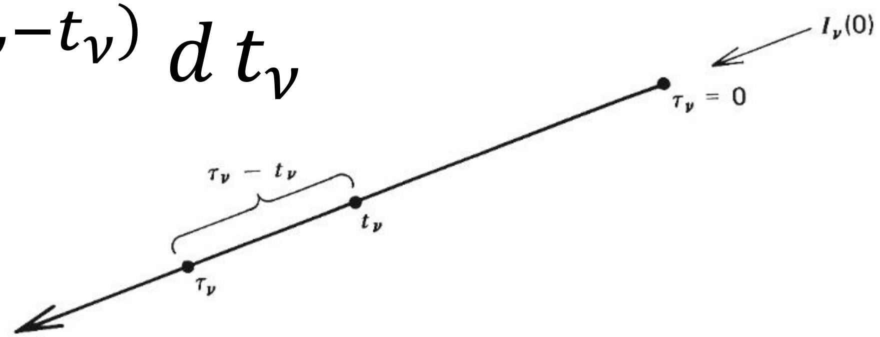

In the atmosphere → no incident radiation, with infinite optical depth

$$\boxed{I_\nu(0,\theta) = \int_0^\infty S_\nu(t_\nu)\, e^{-t_\nu \sec\theta}\, d\,t_\nu \cdot \sec\theta}$$

$$I_\nu(0,\theta) = \int_0^\infty S_\nu(t_\nu)\, e^{-t_\nu \sec\theta} d\, t_\nu \cdot \sec\theta$$

This gives the intensity from the "disk" of the star

At the edge, $\theta \to \pi/2$, $\sec\theta \to \infty$,

$$I_\nu(0,\pi/2) \to 0$$

At the center, $\theta = 0$, $\sec\theta = 1$,

$$I_\nu(0,0) = \int_0^\infty S_\nu(t_\nu)\, e^{-t_\nu} d\, t_\nu$$

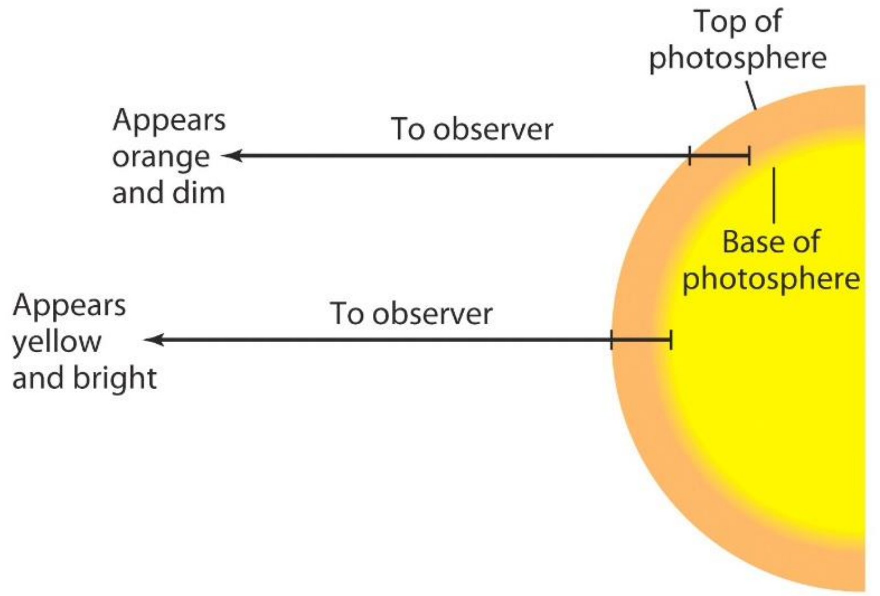

→ **limb darkening**

The limb of a stellar disk is dimmer than to the center (on the average, hotter seen to the same optical depth) .

For the Sun, $I_{\mathrm{limb}} \approx$ 80% $I_{\mathrm{disk\ center}}$ @550 nm;
dimmer in the blue

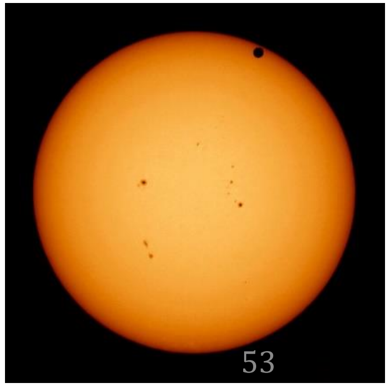

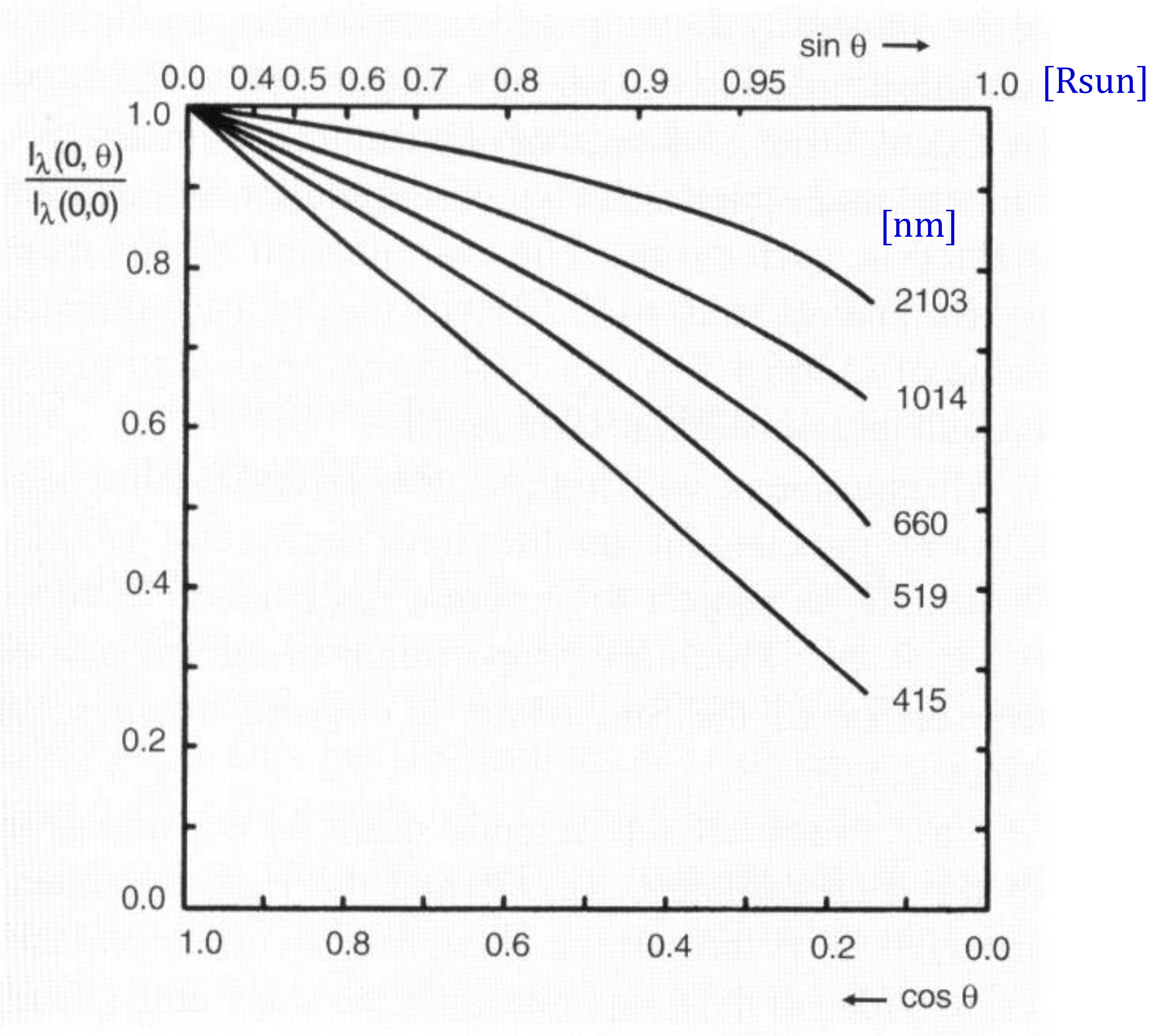
sin θ →
0.0 0.4 0.5 0.6 0.7 0.8 0.9 0.95 1.0
[Rsun]
$\frac{I_\lambda(0,\theta)}{I_\lambda(0,0)}$
1.0 0.8 0.6 0.4 0.2 0.0
[nm]
2103
1014
660
519
415
1.0 0.8 0.6 0.4 0.2 0.0
← cos θ

Unsold, p.169

$$I_\nu(0,\theta) = \int_0^\infty S_\nu(t_\nu)\, e^{-t_\nu \sec\theta} d\, t_\nu \cdot \sec\theta$$

Approximate the source function by Taylor expansion,

$S_\nu \approx a_\nu + b_\nu\, \tau_\nu \longrightarrow I_\nu(0,\theta) = a_\nu + b_\nu\, \cos\theta$

So $\boxed{I_\nu(\theta) = S_\nu(\tau_\nu = \cos\theta)}$. (**Eddington-Barbier relation**)

The specific intensity on the surface at position θ is the source function at the optical depth θ.

The effect of limb darkening observable in details for the Sun → measuring I_ν across the solar disk → mapping the depth dependence of S_ν → to probe the structure in the atmosphere

Seen also in some eclipsing binaries, or in large stars by interferometry, or in exoplanet transits.

de Boer & Seggewiss

Recall that flux $F_\nu = \int I_\nu \cos\theta \, \mathrm{d}\nu \, \mathrm{d}\omega$

$$= \int_0^1 (a_\nu + b_\nu \cos\theta) \cos\theta \, \mathrm{d}\cos\theta = a_\nu + \frac{2}{3} b_\nu$$

$$\boxed{\mathrm{F}_\nu = S_\nu(\tau_\nu = 2/3)}$$

Assuming LTE, so $S_\nu = B_\nu$, and a gray atmosphere ($F(0) = \sigma T_{\mathrm{eff}}^4$), then $F_\nu(0) = \pi B_\nu(T)(\tau = 2/3) = \sigma T_{\mathrm{eff}}^4$

This means $\boxed{T_{\mathrm{eff}} = T(\tau = 2/3)}$

So the effective temperature of the stellar surface is the temperature at the optical depth 2/3.

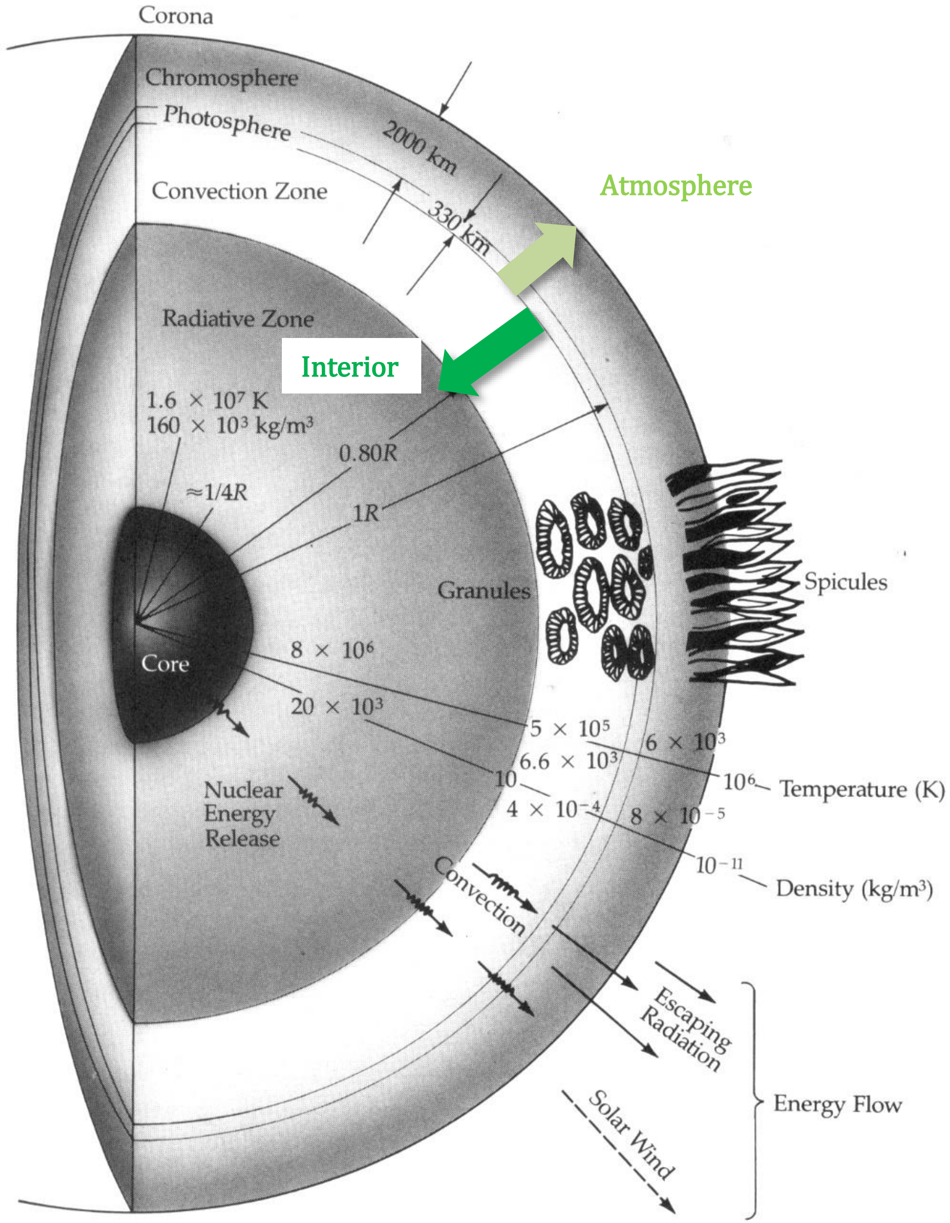

Solar Structure

Thermonuclear fusion $\lesssim 0.25\ R_\odot$

Radiative core up to $\approx 0.80\ R_\odot$

Convective envelope

Outer radiative layer

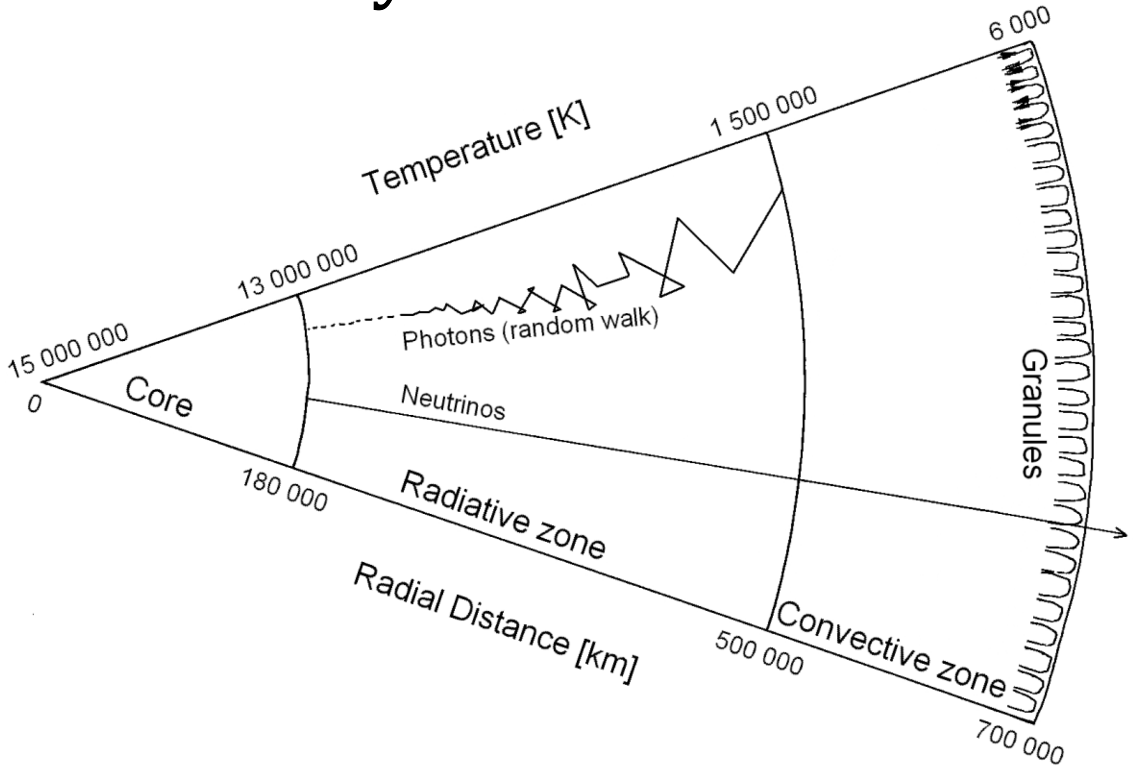

$$T_{\mathrm{eff}} = T(\tau = 2/3)$$

Table 7.4. Models of stellar atmospheres after R. L. Kurucz (1979) for the solar element mixture and different effective temperatures T_{eff} and gravitational accelerations g. Line absorption is taken into account by using distribution functions; the optical depth τ_0 refers to κ_λ at $\lambda = 500$ nm, $\bar{\tau}$ to the Rosseland average $\bar{\kappa}$

Sun G2 V, $T_{\mathrm{eff}} = 5770$ K, $g = 274\ \mathrm{m\,s^{-2}}$

$\bar{\tau}$	τ_0	T [K]	P_g [Pa]	P_e [Pa]
10^{-3}	$1.1 \cdot 10^{-3}$	4485	$3.46 \cdot 10^2$	$2.84 \cdot 10^{-2}$
0.01	0.01	4710	$1.29 \cdot 10^3$	$1.03 \cdot 10^{-1}$
0.10	0.09	5070	$4.36 \cdot 10^3$	$3.78 \cdot 10^{-1}$
0.22	0.19	5300	$6.51 \cdot 10^3$	$6.43 \cdot 10^{-1}$
0.47	0.40	5675	$9.55 \cdot 10^3$	1.34
1.0	0.84	6300	$1.29 \cdot 10^4$	4.77
2.2	1.8	7085	$1.52 \cdot 10^4$	$2.13 \cdot 10^1$
4.7	3.5	7675	$1.71 \cdot 10^4$	$5.86 \cdot 10^1$
10	7.1	8180	$1.89 \cdot 10^4$	$1.27 \cdot 10^2$

α Lyr A0 V, $T_{\mathrm{eff}} = 9400$ K, $g = 89\ \mathrm{m\,s^{-2}}$

$\bar{\tau}$	τ_0	T [K]	P_g [Pa]	P_e [Pa]
10^{-3}	$0.6 \cdot 10^{-3}$	7140	6.52	$4.31 \cdot 10^{-1}$
0.01	$0.5 \cdot 10^{-2}$	7510	$2.70 \cdot 10^1$	1.61
0.10	0.05	8150	$9.13 \cdot 10^1$	7.33
0.22	0.11	8590	$1.22 \cdot 10^2$	$1.40 \cdot 10^1$
0.47	0.24	9240	$1.53 \cdot 10^2$	$2.94 \cdot 10^1$
1.0	0.53	10 190	$1.79 \cdot 10^2$	$5.81 \cdot 10^1$
2.2	1.3	11 560	$2.12 \cdot 10^2$	$9.21 \cdot 10^1$
4.7	3.6	13 480	$2.99 \cdot 10^2$	$1.40 \cdot 10^2$
10	11.5	16 000	$5.81 \cdot 10^2$	$2.77 \cdot 10^2$

B0 V, $T_{\mathrm{eff}} = 30\,000$ K, $g = 100\ \mathrm{m\,s^{-2}}$ [a]

$\bar{\tau}$	τ_0	T [K]	P_g [Pa]	P_e [Pa]
10^{-3}	$0.8 \cdot 10^{-3}$	19 680	2.13	1.07
0.01	$0.9 \cdot 10^{-2}$	21 450	$1.60 \cdot 10^1$	7.98
0.10	0.14	24 880	$1.01 \cdot 10^2$	$5.03 \cdot 10^1$
0.22	0.37	27 030	$1.86 \cdot 10^2$	$9.31 \cdot 10^1$
0.47	0.92	29 840	$3.33 \cdot 10^2$	$1.66 \cdot 10^2$
1.0	2.2	33 490	$5.87 \cdot 10^2$	$2.95 \cdot 10^2$
2.2	5.5	38 310	$1.04 \cdot 10^3$	$5.29 \cdot 10^2$
4.7	13.3	43 940	$1.81 \cdot 10^3$	$9.43 \cdot 10^2$
10	37	51 310	$3.60 \cdot 10^3$	$1.88 \cdot 10^3$

[a] Corresponds roughly to the parameters of τ Sco (B0 V) $T_{\mathrm{eff}} = 31\,500$ K and $g = 140\ \mathrm{m\,s^{-2}}$.

Model stellar atmospheres by R. L. Kurucz (1979) for solar abundance, and for different T_{eff} and g

Unsold

ATLAS:
A COMPUTER PROGRAM FOR CALCULATING
MODEL STELLAR ATMOSPHERES

Robert L. Kurucz

1. INTRODUCTION

The calculation of a model atmosphere is a straightforward process once several assumptions and approximations have been made to simplify the problem physically and computationally. We simplify the problem as follows:

A. The atmosphere is in a steady state.

B. The flux of energy is constant with depth in the atmosphere since the energy source for the star lies far below the atmosphere and since no energy comes into the atmosphere from above. The flux is usually specified by an effective temperature such that flux = σT_{eff}^4, σ = 5.6697E-5.

C. The atmosphere is homogeneous except in the normal direction. We ignore granules, spicules, cells, spots, magnetic fields, etc.

D. The atmosphere is thin relative to the radius of the star, so we can consider plane layers instead of concentric shells.

Kurucz (1970)
SAO Special Report #309

E. There is no relative motion of the layers in the normal direction and no net acceleration of the atmosphere, so the pressure balances the gravitational attraction,

$$\rho \frac{d^2 r}{dt^2} = -\rho g + \frac{dP}{dr} = 0 \quad . \tag{1.1}$$

Here ρ is the density and g is the gravitational acceleration, which is approximately constant because the atmosphere is thin,

$$g = \frac{GM_*}{R_*^2} \quad ,$$

with M_* and R_* the mass and radius of the star.

F. The atomic abundances are specified and constant throughout the atmosphere.

Given these assumptions, we go through an iteration process to find the parameters that describe the model atmosphere. We guess the temperature at a set of depth points in the atmosphere and calculate the pressure, number densities, and opacity at each point. From these quantities we determine the radiation field and convective flux at each point. The total flux does not, in general, equal the prescribed constant flux, so we change the temperature at each point according to a "temperature correction" scheme. We repeat the whole process with successive temperature distributions until the total flux is constant to within a small error.

THE ASTROPHYSICAL JOURNAL SUPPLEMENT SERIES, 40:1–340, 1979 May
© 1979. The American Astronomical Society. All rights reserved. Printed in U.S.A.

MODEL ATMOSPHERES FOR G, F, A, B, AND O STARS

ROBERT L. KURUCZ*
Harvard-Smithsonian Center for Astrophysics
Received 1978 July 24; accepted 1978 October 11

ABSTRACT

A grid of LTE model atmospheres is presented for effective temperatures ranging from 5500 to 50,000 K, for gravities from the main sequence down to the radiation pressure limit, for abundances solar, 1/10 solar, and 1/100 solar. The models were computed by use of a statistical distribution-function representation of the opacity of almost 10^6 atomic lines. For each model we tabulate the temperature structure, fluxes, *UBV* and *uvby* colors, bolometric correction, and Balmer line profiles. The solar abundance models are compared to narrow, intermediate (by Relyea and Kurucz), and wide (by Relyea and Kurucz and by Buser and Kurucz) band photometry and are found to be in good agreement with the observations for effective temperatures above 8000 K. Excellent agreement exists with the spectrophotometry and Balmer line profiles of Vega. A small systematic error in the colors of late A and F stars is probably due to an overestimate of convection in weakly convective models. This error does not seem to affect greatly the use of the predicted colors for differential studies. The solar model has approximately a 2% error in the *V* flux because molecular lines were not included.

Kurucz (1979)

TABLE 4

The Models

TEFF 5500. LOG G 0.00 LOG ABUND .00 CONVECTIVE

	MASS	TAU ROSS	TAU 500	X	T	P	NE	NA	RHO	KAPPA ROSS	KAPPA 500	P RAD	ACC RAD	CONV FRAC
1	-.38761	0.0000	0.0000	0.0000	3000.3	-.3893	7.7323	11.9934	-11.6635	-4.1046	-3.3399	.0865	-2.6844	-27.0123
2	-.22215	-4.3268	-3.5621	10.9100	3765.6	-.2238	8.0766	12.0603	-11.5966	-4.1046	-3.3399	.0866	-2.8477	-29.3451
3	-.06172	-4.1624	-3.4012	11.2337	3816.9	-.0632	8.2353	12.2150	-11.4419	-4.0797	-3.3373	.0868	-2.8742	0.0000
4	.09200	-3.9979	-3.2464	11.4124	3867.2	.0906	8.3877	12.3631	-11.2938	-4.0517	-3.3340	.0869	-2.8817	0.0000
5	.24067	-3.8327	-3.0958	11.5345	3915.9	.2393	8.5353	12.5064	-11.1505	-4.0203	-3.3298	.0872	-2.8864	0.0000
6	.38470	-3.6673	-2.9491	11.6280	3964.2	.3835	8.6790	12.6452	-11.0117	-3.9846	-3.3244	.0875	-2.8897	0.0000
7	.52497	-3.5007	-2.8053	11.7038	4013.3	.5239	8.8195	12.7803	-10.8766	-3.9435	-3.3177	.0879	-2.8824	0.0000
8	.65991	-3.3347	-2.6658	11.7668	4064.7	.6588	8.9565	12.9096	-10.7472	-3.8969	-3.3092	.0885	-2.8735	0.0000
9	.78968	-3.1691	-2.5302	11.8205	4118.0	.7887	9.0903	13.0339	-10.6230	-3.8447	-3.2986	.0892	-2.8674	0.0000
10	.91489	-3.0032	-2.3979	11.8672	4172.3	.9139	9.2217	13.1534	-10.5034	-3.7875	-3.2856	.0902	-2.8623	0.0000
11	1.03612	-2.8363	-2.2678	11.9086	4227.2	1.0350	9.3508	13.2689	-10.3880	-3.7254	-3.2698	.0915	-2.8573	0.0000
12	1.15290	-2.6693	-2.1403	11.9455	4282.3	1.1520	9.4776	13.3802	-10.2767	-3.6586	-3.2507	.0932	-2.8511	0.0000
13	1.26459	-2.5035	-2.0158	11.9785	4336.6	1.2636	9.6009	13.4864	-10.1705	-3.5887	-3.2281	.0952	-2.8435	0.0000
14	1.37272	-2.3372	-1.8923	12.0086	4390.3	1.3720	9.7221	13.5894	-10.0675	-3.5151	-3.2015	.0979	-2.8300	0.0000
15	1.47727	-2.1706	-1.7695	12.0361	4444.0	1.4765	9.8415	13.6887	-9.9682	-3.4382	-3.1705	.1012	-2.8094	0.0000
16	1.57875	-2.0033	-1.6466	12.0616	4498.2	1.5781	9.9599	13.7849	-9.8720	-3.3578	-3.1347	.1056	-2.7844	0.0000
17	1.67655	-1.8368	-1.5239	12.0851	4552.7	1.6759	10.0766	13.8775	-9.7794	-3.2751	-3.0940	.1111	-2.7501	0.0000
18	1.77126	-1.6701	-1.4005	12.1069	4609.4	1.7706	10.1937	13.9668	-9.6901	-3.1886	-3.0477	.1183	-2.7084	0.0000
19	1.86290	-1.5033	-1.2758	12.1273	4669.6	1.8622	10.3128	14.0528	-9.6041	-3.0981	-2.9948	.1277	-2.6603	0.0000
20	1.95141	-1.3361	-1.1494	12.1463	4734.2	1.9507	10.4347	14.1353	-9.5216	-3.0030	-2.9349	.1400	-2.6041	0.0000
21	2.03635	-1.1690	-1.0214	12.1641	4805.4	2.0354	10.5618	14.2136	-9.4433	-2.9014	-2.8664	.1560	-2.5369	0.0000
22	2.11679	-1.0025	-.8921	12.1806	4887.2	2.1159	10.6983	14.2867	-9.3702	-2.7899	-2.7866	.1770	-2.4535	0.0000
23	2.19226	-.8352	-.7606	12.1957	4985.6	2.1912	10.8505	14.3533	-9.3036	-2.6635	-2.6908	.2045	-2.3524	0.0000
24	2.26091	-.6684	-.6278	12.2094	5104.6	2.2598	11.0228	14.4116	-9.2452	-2.5191	-2.5752	.2399	-2.2302	0.0000
25	2.32138	-.5017	-.4937	12.2214	5252.7	2.3201	11.2225	14.4595	-9.1974	-2.3488	-2.4330	.2852	-2.0776	0.0000
26	2.37239	-.3348	-.3581	12.2315	5436.9	2.3707	11.4538	14.4949	-9.1620	-2.1474	-2.2590	.3423	-1.8891	-15.8934
27	2.41322	-.1676	-.2211	12.2398	5665.4	2.4111	11.7184	14.5171	-9.1397	-1.9119	-2.0496	.4129	-1.6641	-11.7676
28	2.44392	.0003	-.0827	12.2462	5949.4	2.4411	12.0175	14.5252	-9.1317	-1.6340	-1.7996	.4984	-1.3922	-9.4069
29	2.46531	.1680	.0554	12.2509	6289.4	2.4613	12.3377	14.5198	-9.1370	-1.3151	-1.5122	.5997	-1.0676	-6.8868
30	[illegible]	[illegible]	[illegible]	[illegible]	[illegible]	[illegible]	[illegible]	[illegible]	[illegible]	[illegible]	[illegible]	[illegible]	[illegible]	[illegible]

Kurucz (1979) ApJS, 40, 1—340

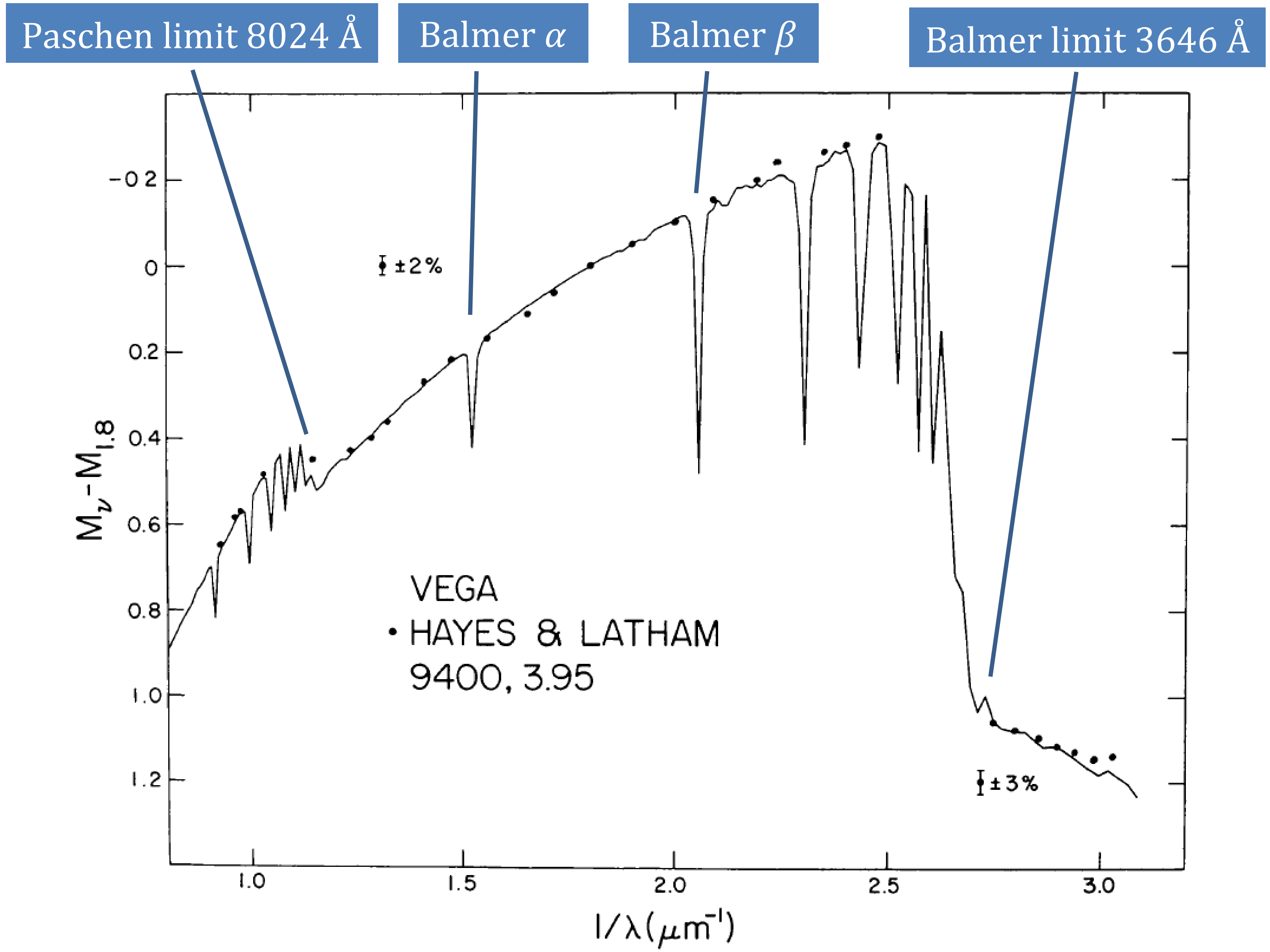

FIG. 26.—Comparison of the colors of the 9400, 3.95 model with the recalibration of Vega by Hayes and Latham (1975). Error bars for the observations are indicated.

Kurucz (1979)

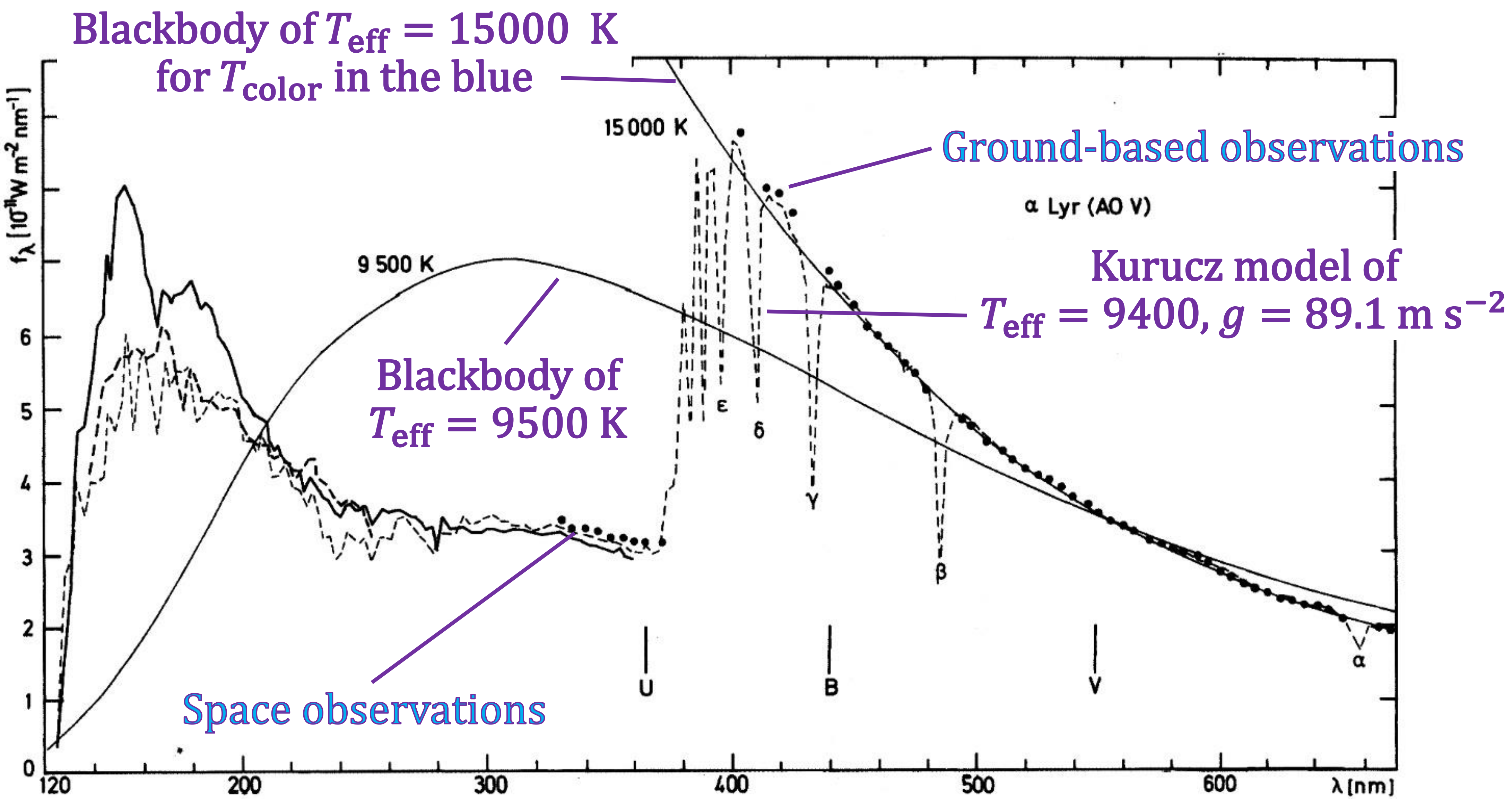

The energy distribution of Vega

Unsold, Fig 6.7

Line Broadening

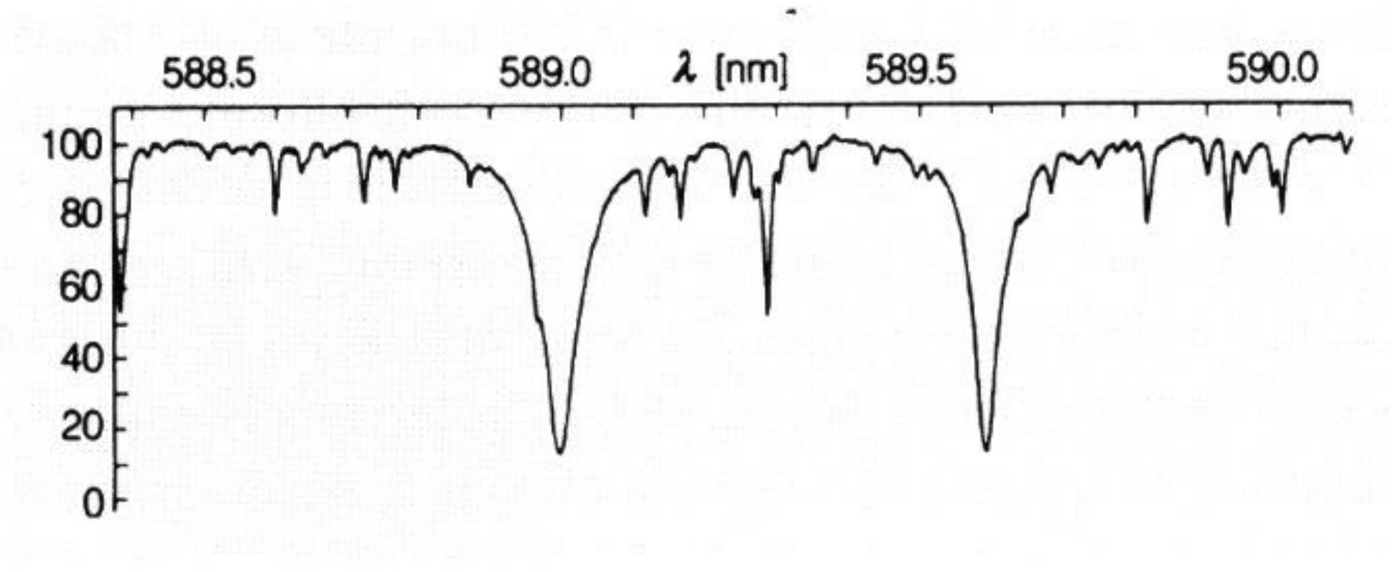

Natural Broadening

QM Heisenberg energy-time uncertainty principle

$$\Delta E \, \Delta t \geq h$$

That is, the energy of a given state cannot be specified more accurately than this → $\Delta \nu \approx 1/\,\Delta t$. Typically $\Delta t \approx 10^{-8}$ s (recall Einstein's A coefficients), so the natural width of a line $\approx 5 \times 10^{-5}$ nm. Meta-stable states have even much narrow lines.

Thermal Doppler Broadening

Particle motion along the line of sight → Doppler shift

$$\langle mv^2/2 \rangle = 3\,kT/2$$

At a given temperature, a spectral line due to a heavier element is narrower.

At 6000 K, H moves at $v \approx 12\ \mathrm{km\ s^{-1}}$, leading to a fractional Doppler broadening $\Delta\lambda/\lambda \approx v/c \approx 4 \times 10^{-5}$, so the H$\alpha$ line (656.3 nm) is broadened by 0.025 nm.

The broadening is temperature and composition dependent.

Zeeman Broadening

Energy levels spilt to 3 or more sublevels in a magnetic field
→ **Zeeman effect** (Pieter Zeeman)

Spectral lines closed spaced ($\propto$ **B** strength), so difficult to resolve
→ line broadened

Collisional Broadening

Energy levels shifted by nearby particles, especially ions and electrons ("**Stark Effect**" due to **E** field); also called pressure broadening. Density dependent

---

Additional broadening mechanisms: rotation, expanding, turbulence, ..., etc.

Line Profile

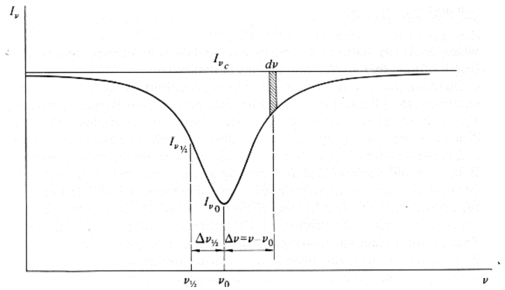

- The details of a line profile: absorption coefficient as a function of frequency within the line
- Superimposed on the Doppler profile (macroscopic motion of particles) are the radiative and collisional damping effects.

An atom → a dipole; the electron oscillates when interacting with an incident EM wave

In general, $\underbrace{m\ddot{r}}_{\text{Force on the electron}} = \underbrace{-mr\omega_0^2}_{\text{Restoring force}} \underbrace{- m\gamma\dot{r}}_{\text{Damping force}} \underbrace{- eE_0\, e^{i\omega t}}_{\text{Force by EM wave}}$

Novotny, p.199

Lorentz (damping) profile

$$\boxed{\phi(\Delta\nu) = \frac{\gamma}{(2\pi\Delta\nu)^2 + (\gamma/2)^2}}$$

Classical treatment

Atom absorbing a photon → excited → e^- oscillates as a dipole

Equation of motion: $m\ddot{r} = -4\pi^2 r \nu_0^2$

Such a dipole radiates with power $\mathbb{P} = \frac{2}{3}\frac{e^2}{c^3}|\ddot{r}|^2$

Energy is radiated away → damping force to slow down the e^-

The force is $\mathcal{F} = \frac{2}{3}\frac{e^2}{c^3}|\dddot{r}|^2$, and for a small damping

→ a simple harmonic motion (around ν_0)…

Scattering by dust or molecules → harmonically bound charge, oscillating at a natural frequency ω_0. The incident field $\boldsymbol{E} = \boldsymbol{E}_0 \cos(\boldsymbol{k}\cdot\boldsymbol{r} - \omega t + \alpha)$ forces the oscillator to vibrate at a different frequency ω.

The acceleration is $m\ddot{\boldsymbol{r}} = e\boldsymbol{E}$.

The dipole moment by the displacement of the charge, $\boldsymbol{d} = e\boldsymbol{r}$, $\ddot{\boldsymbol{d}} = e^2\boldsymbol{E}/m$

The equation of motion of the forced oscillation is $\ddot{\boldsymbol{r}} + \omega_0^2\boldsymbol{r} = e\boldsymbol{E}/m$.

The solution is $\boldsymbol{r} = \frac{e^2}{m}\boldsymbol{E}\left(\frac{1}{\omega_0^2-\omega^2}\right)$, and $\ddot{\boldsymbol{d}} = e^2\boldsymbol{E}/m\left[\frac{1}{1-(\omega_0^2/\omega^2)}\right]$

The scattering cross section is $\sigma = \frac{\sigma_e}{\left(1-\omega_0^2/\omega^2\right)^2}$

Electrons are strongly bound so $\omega_0 \gg \omega$ in optical wavelengths, so

$$\sigma = \frac{\sigma_e\omega^4}{\omega_0^4}$$

Harwit p. 234

is the **Rayleigh scattering** cross section (this is why the clear sky is blue).

Classically the damping constant $\gamma \approx A$, the transition probability

The effective number of oscillators → **oscillator strength**, relates the spectral line to harmonic electron-oscillators, and is related to the Einstein B coefficient

$$\int_{\text{line}} \sigma_{ij}(\nu)d\nu = \frac{h\nu}{4\pi} B_{ij} = \frac{\pi e^2}{m_e c} f$$

The oscillator strength f, the ratio of

[QM transition rate]/[Classical rate],

is dimensionless, and related to the A coefficient

$$g_j A_{ji} = \frac{8\pi^2 e^2 \nu^2}{m_e c^3} g_i f$$

Equivalent to how many classical oscillators

For Balmer lines, $f(\mathrm{H}\alpha) = 0.641, f(\mathrm{H}\beta) = 0.119, f(\mathrm{H}\gamma) = 0.044$.

Kramers computed the analytic approximation for H,

$$f_{ji} = \frac{-g_i}{g_j} f_{ij} = \frac{2^6}{3\sqrt{3}\,\pi} \frac{1}{g_i} \frac{1}{(1/i^2 - 1/j^2)^3} \frac{g_{bb}}{j^3 i^3}$$

Where g_{bb} is the Kramers-Gaunt factor, or **Gaunt factor**, for the bound-bound transition to <u>correct for the QM effect</u>, and is on the order of unity.

Bower & Deeming

Doppler profile

$$\phi(\Delta\nu) = \frac{1}{\sqrt{\pi}\,\Delta\nu_\mathrm{D}} \exp[-(\Delta\nu/\Delta\nu_\mathrm{D})^2]$$

This has a FWHM of $2\Delta\nu_\mathrm{D}\sqrt{\ln 2}$

$\Delta\nu_\mathrm{D}$ or $\Delta\lambda_\mathrm{D}$ is defined by the most probable speed.

Voigt profile **Doppler core + Damping wings** (convolution)

$$\phi(\Delta\nu) = \int_{-\infty}^{+\infty} \mathcal{L}(\Delta\nu - \Delta\nu')\,\mathcal{D}(\Delta\nu')\,d\Delta\nu'$$

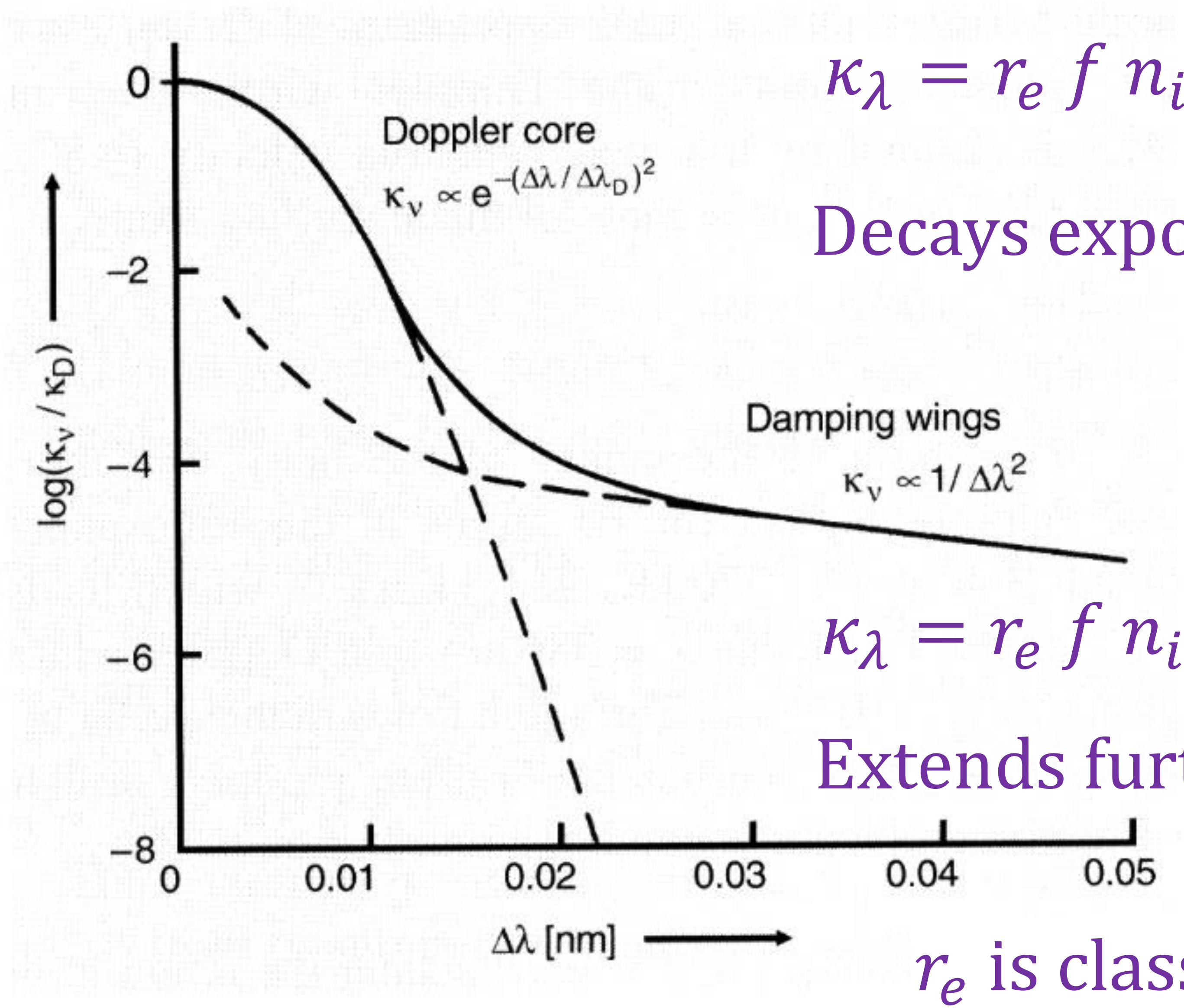

$$\kappa_\lambda = r_e\, f\, n_i \sqrt{\pi}\ \frac{\lambda_0^2}{\Delta\lambda_0} \exp\left[-\left(\frac{\Delta\lambda}{\Delta\lambda_D}\right)^2\right]$$

Decays exponentially

$$\kappa_\lambda = r_e\, f\, n_i \sqrt{\pi}\ \frac{\lambda_0^4}{4\pi c} \frac{\gamma}{(\Delta\lambda)^2}$$

Extends further (wings)

r_e is classical electron radius;
n_i is density at lower level

Unsold

Equivalent Width

Photons of different wavelengths carry different energies. Which line is "stronger" (how much energy is missing in a spectral line)?

→ Compare with local "continuum", i.e., where there is no absorption

$$\phi_\nu = \frac{I_c - I_\lambda}{I_c}$$

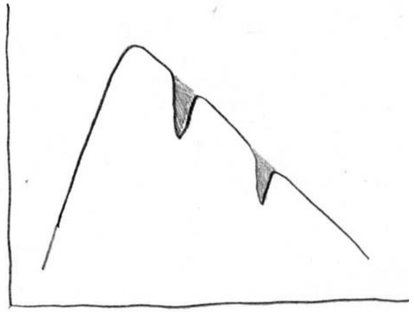

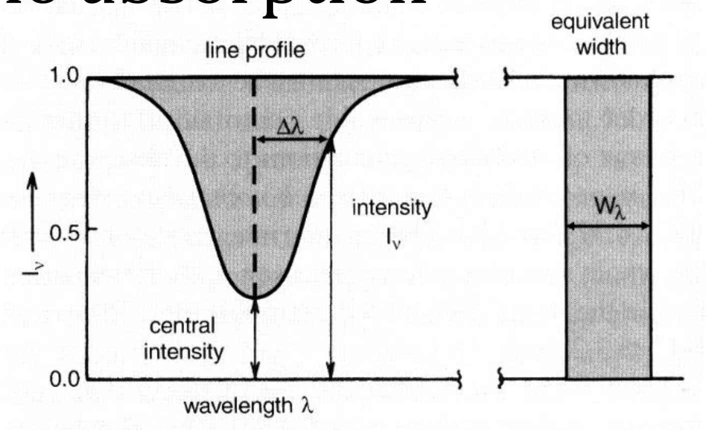

$$W_\lambda = \int_{-\infty}^{\infty} \frac{I_c - I_\lambda}{I_c}\, d\lambda = \int 1 - e^{-\tau_\lambda}\, d\lambda$$

$$\frac{W_\lambda}{\lambda} = \frac{W_\nu}{\nu} = \frac{W_v}{c}$$

is the **equivalent width** (W), which measures the absorption (strength) of a spectral line, where I_λ is the line profile, and I_c is the continuum (at the same λ). W in unit of [Å] or [mÅ]; traditionally negative for emission lines.

Recall, for an absorption line,

$$I_\nu(\tau_\nu) = I_\nu(0)\, e^{-\tau_\nu}$$

So for an optically thin medium (physically thin or of a low density), $\tau_\nu \ll 1 \rightarrow \frac{I_\nu(\text{observed})}{I_\nu(0)} \approx \tau_\nu$

$$\sigma_\nu = \left(\frac{\pi e^2}{mc}\right) f \phi_\nu \qquad\qquad \sigma_\nu d\nu = \sigma_\lambda d\lambda$$

$\tau_\nu = \kappa_\nu ds \; = n\, \sigma_\nu\, ds = N\, \sigma_\nu$, where N is the column density

$$\tau_\lambda = N \left(\frac{\pi e^2}{mc^2}\right) f\, \lambda_0^2\, \phi_\nu$$

(1) For a weak line ($\tau_\lambda \ll 1$)

$$W_\lambda = \int \tau_\lambda\, d\lambda = N \left(\frac{\pi e^2}{mc^2}\right) f \lambda_0^2 \propto\; N f$$

The equivalent width measures directly the number of absorbers along the line of sight.

Or

$$\frac{W_\lambda}{\lambda\,[\mathrm{cm}]} = N \left(\frac{\pi e^2}{mc^2}\right) f \lambda_0 = 8.85 \times 10^{-13}\, N_i\, [\mathrm{cm}^{-2}]\, f_{12}$$

Spitzer

(2) For a strong line ($\tau_\lambda \gg 1$), damping wings dominate

$$W_\lambda \propto \sqrt{Nf}$$

(3) For an intermediate case

$$W_\lambda \propto \sqrt{\ln Nf}$$

Line strength (equivalent width)
→ abundance

Curve of growth

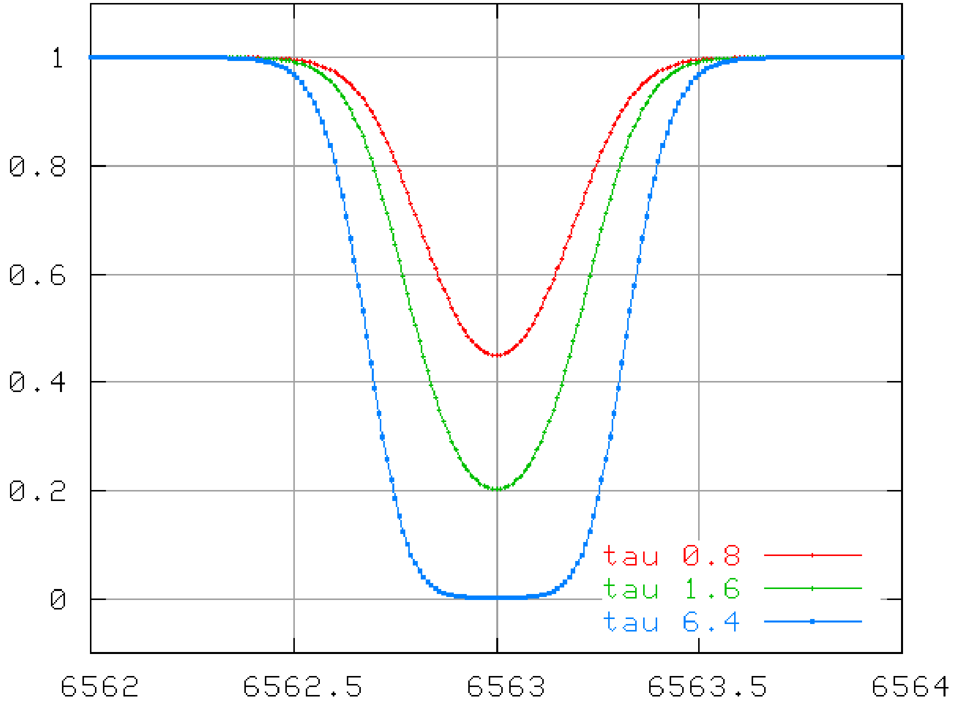

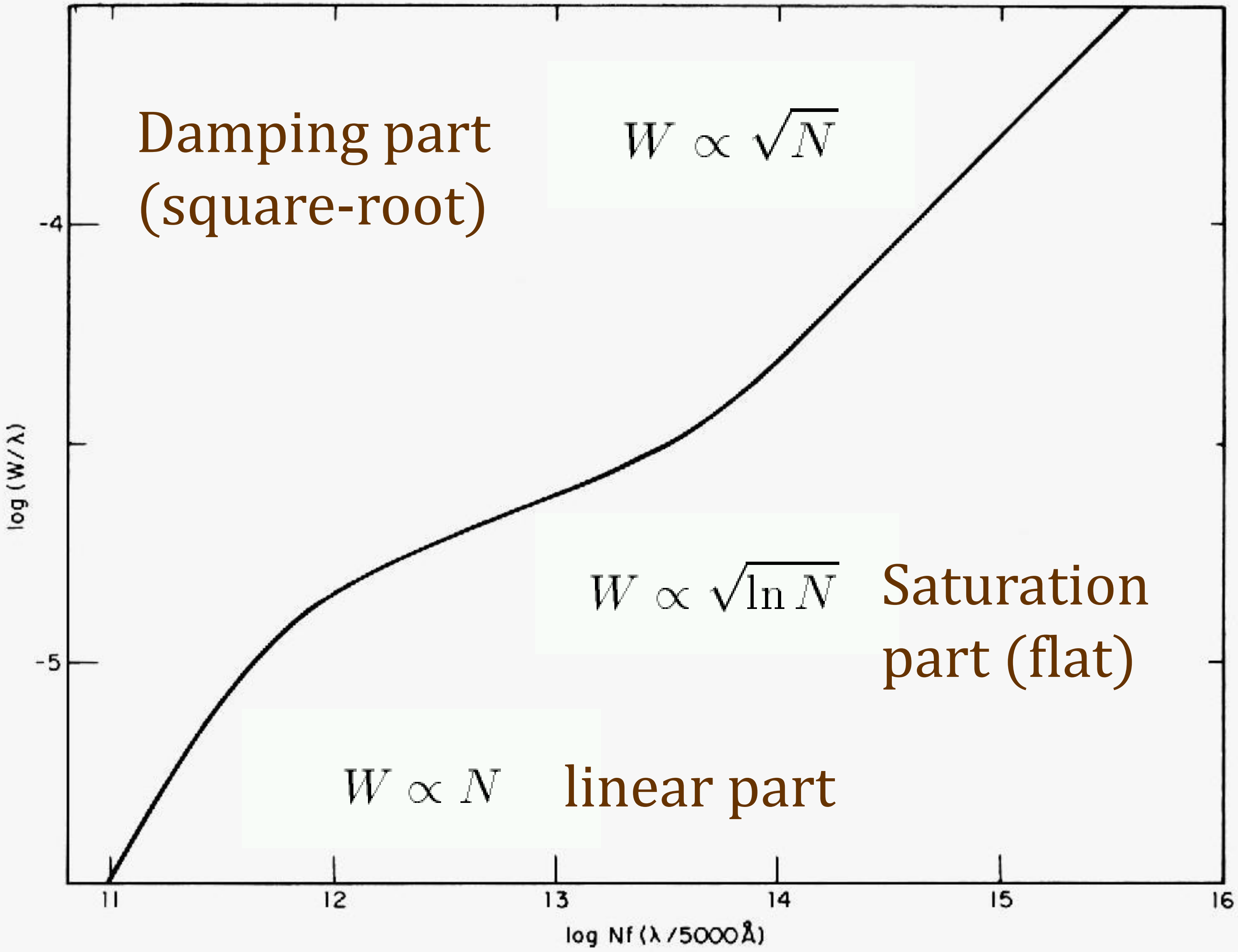

Figure 9.22 A general curve of growth for the Sun. (Figure from Aller, *Atoms, Stars, and Nebulae*, Revised Edition, Harvard University Press, Cambridge, MA, 1971.)

Amount of absorbers → line profile changes and equivalent width changes

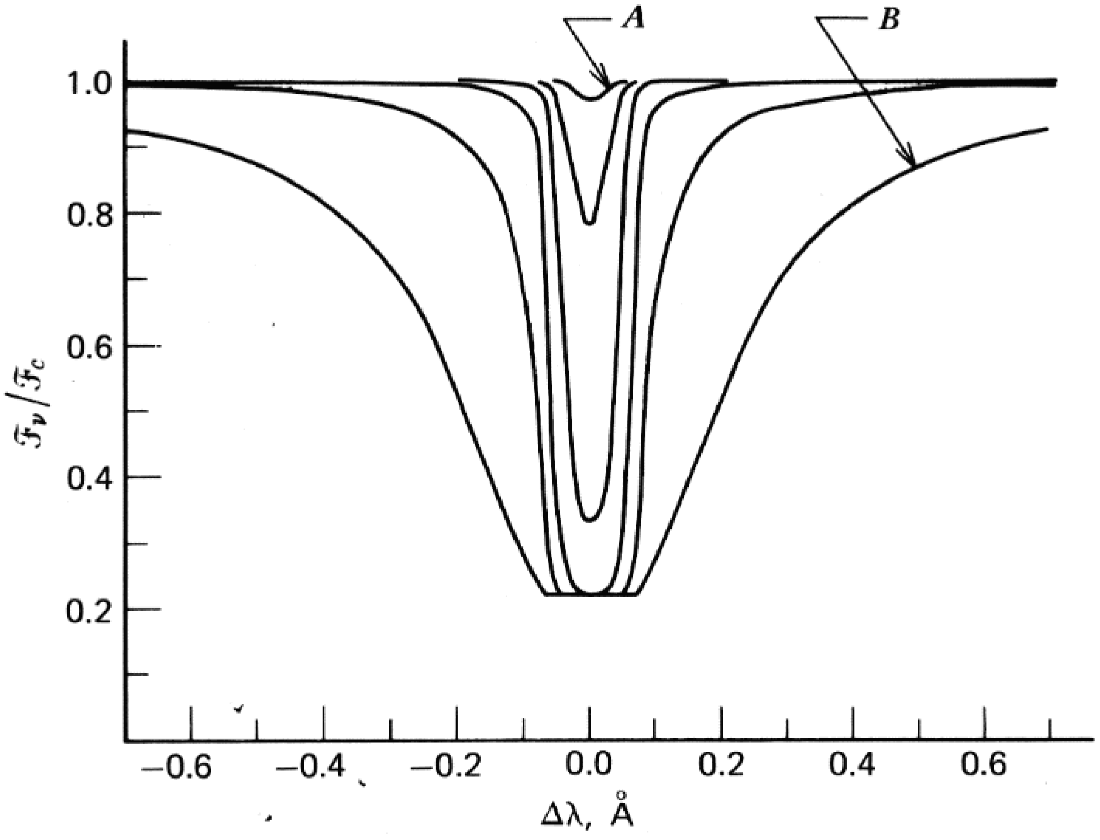

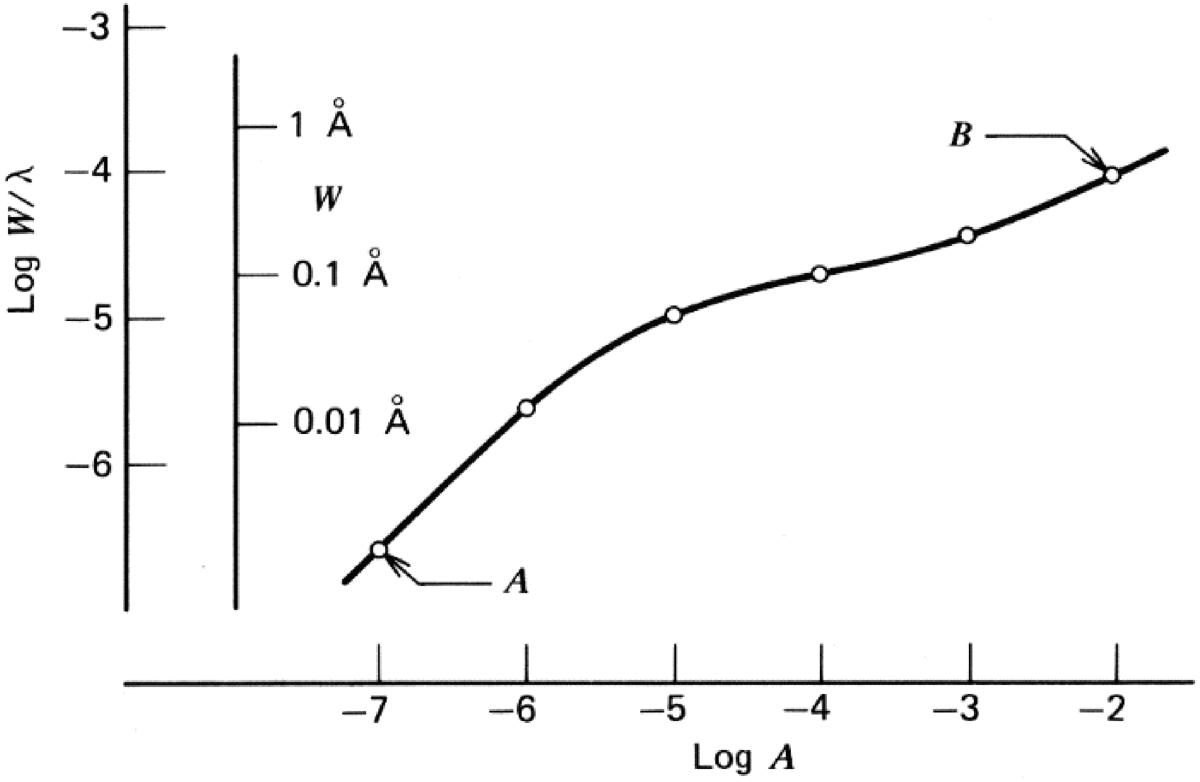

Gray Fig. 13.12

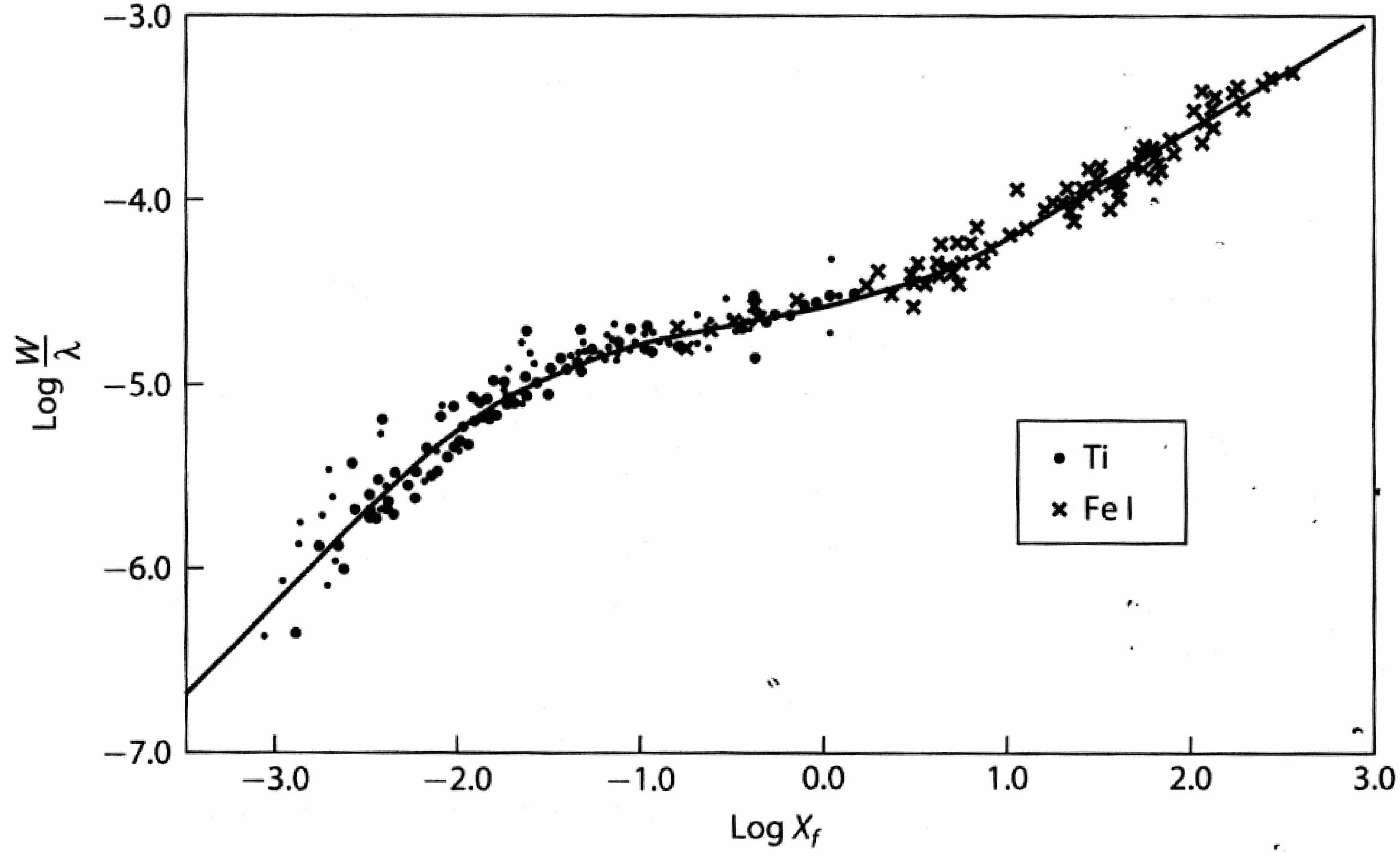

Figure 17.4 An empirical curve of growth. X_f in this figure $\equiv \beta_0$ defined above. From [1179].